Supporting Information for

Di-Cobalt Catalysts for the Copolymerization of CO_2 and Cyclohexene Oxide: Evidence for a Dinuclear Mechanism?

Michael R. Kember, Fabian Jutz, Antoine Buchard, Andrew J.P. White, Charlotte K. Williams*

Department of Chemistry, Imperial College London, London, SW7 2AZ, UK.

Corresponding author email address: c.k.williams@imperial.ac.uk

Experimental Section

Materials and Methods

The syntheses of H_2L^1 was previously reported.[1] The syntheses of all cobalt complexes were conducted under a nitrogen atmosphere, using either standard anaerobic techniques or in a nitrogen filled glovebox. All solvents and reagents were obtained from commercial sources (Aldrich and Strem). THF and hexane were distilled from sodium, thoroughly de-gassed and stored under nitrogen. Cyclohexene oxide (CHO) and methylene chloride were distilled from CaH_2, thoroughly de-gassed and stored under nitrogen. Research grade carbon dioxide was used for copolymerization studies.

^1H and $^{13}C\{^1H\}$ NMR spectra were performed on a Bruker AV-400 instrument, unless otherwise stated. All mass spectrometry measurements were performed using a Fisons Analytical (VG) Autospec spectrometer. MALDI-ToF mass spectrometry measurements were carried out at the National Mass Spectrometry Service Centre at Swansea University. Elemental analyses were determined by Mr Stephen Boyer at London Metropolitan University, North Campus, Holloway Road, London, N7. SEC data were collected using a Polymer labs PL GPC-50 instrument, with THF as the eluent, at a flow rate of 1mL min^{-1}. Two Polymer labs Mixed D columns were used in series. Narrow M_w polystyrene standards were used to calibrate the instrument. In-situ Infrared spectroscopy measurements were taken using a Mettler Toledo ReactIR 4000 instrument with a diamond tipped probe on a 9.5 mm × 2 m silver halide fibre optic cable.

Synthesis of **1a/b**

H_2L^1 (0.3 g, 0.54 mmol) was dissolved in THF (10 mL) in a Schlenk tube. CoX_2 (1.08 mmol) was added to the solution and left to stir for 16 hours at 25 °C, after which the solution turned brown-green. The solvent was removed *in vacuo*, after which the product was dried under vacuum for several hours.

1a (0.57 g, 0.46 mmol, 85 %): *m/z*: (LSI^+): 795 (100 %, $[L^1Co_2I]^+$). Anal. Calc. for $C_{34}H_{54}Co_3I_4N_4O_2$: C, 36.06; H, 4.41; N, 4.54. Found: C, 32.94; H, 4.48; N, 4.31.

1b (0.46 g, 0.44 mmol, 82 %): *m/z*: (LSI^+): 747 (100 %, $[L^1Co_2Br]^+$). Anal. Calc. for $C_{34}H_{54}Co_3Br_4N_4O_2$: C, 38.28; H, 5.10, N, 5.25. Found: C, 38.41; H, 5.15; N, 5.13.

***Synthesis of* K[($L^1Co_2Cl_2$)$_2$Cl]-2**

H_2L^1 (0.40 g, 0.72 mmol) was dissolved in THF (10 mL) and transferred into a Schlenk tube containing KH (0.87 g, 2.20 mmol) and cooled to -78 °C, under nitrogen. The suspension was allowed to warm to room temperature and left to stir for 1 hour. Any excess KH was filtered, and $CoCl_2$ (0.19 g, 1.44 mmol) was added to the solution, slowly. The solution was left to stir overnight, producing a purple solution. The solvent was removed, *in vacuo*, and the pink powder was dried, under vacuum, for several hours (0.48 g, 0.31 mmol, 85 %).
m/z: (LSI$^+$): 703 (100 %, [$L^1Co_2Cl]^+$). Anal. Calc. for $C_{68}H_{108}Cl_5Co_4KN_8O_4$: C, 52.57; H, 7.01; N, 7.21. Found: C, 52.52; H, 6.94; N, 7.23. UV-Vis λ_{max}/nm (ε/dm^{3}mol^{-1}cm^{-1}): 475 (67.2), 540 (63.9), 570 (55.7), 700 (16.1).

***General procedure for the synthesis of* 3a-c**

H_2L^1 (0.25 g, 0.45 mmol) was dissolved in THF (10 mL) in a Schlenk tube. The base (0.9 mmol) was added to the solution and left to stir for 1 hour. $CoCl_2$ (0.12 g, 0.9 mmol) was added to the solution, slowly, to prevent formation of [$L^1Co_3Cl_4$], and the solution was left stirring overnight, after which a purple solution was found, with a white precipitate. The precipitate was filtered and the solvent removed, *in vacuo*, to yield a pink powder which was dried, under vacuum, for several hours.

3a (0.33 g, 0.38 mmol, 84 %): *m/z* (LSI$^+$): 102 (100 %, $[HNEt_3]^+$), (ESI$^-$): 803 (100 %, $[L^1Co_2(HCO_2)_3]^-$), 793 (20 %, $[L^1Co_2Cl(HCO_2)_2]^-$). Anal. Calc. for $C_{40}H_{70}Cl_3Co_2N_5O_2$: C, 54.77; H, 8.04; N, 7.98. Found: C, 54.84; H, 7.98; N, 8.02. UV-Vis λ_{max}/nm (ε/dm^{3}mol^{-1}cm^{-1}): 473 (67.9), 541 (61.8), 565 (52.3).

3b (0.33 g, 0.0.36 mmol, 79 %): *m/z*: (LSI$^+$): 153 (100 %, [H-DBU]$^+$), (ESI$^-$): 803 (100 %, $[L^1Co_2(HCO_2)_3]^-$), 793 (25 %, $[L^1Co_2Cl(HCO_2)_2]^-$). Anal. Calc. for $C_{43}H_{71}Cl_3Co_2N_6O_2$: C, 55.64; H, 7.71; N, 9.05. Found: C, 55.69; H, 7.79; N, 9.08.

3c (0.31 g, 0.33 mmol, 74 %): *m/z*: (LSI$^+$): 154 (100 %, [H-MTBD]$^+$), *m/z* (ESI$^-$) 803 (100 %, $[L^1Co_2(HCO_2)_3]^-$), 793 (20 %, $[L^1Co_2Cl(HCO_2)_2]^-$). Anal. Calc. for $C_{42}H_{70}Cl_3Co_2N_7O_2$: C, 54.28; H, 7.59; N, 10.55%. Found: C, 54.16; H, 7.65; N, 10.41%.

***General procedure for the synthesis of* 4a-c**

H_2L^1 (0.40 g, 0.72 mmol) was dissolved in THF (10 mL) and transferred into a Schlenk tube containing KH (0.87 g, 2.20 mmol) and cooled to -78 °C, under nitrogen. The suspension was allowed to warm to room temperature and left to stir for 1 hour. Any excess KH was filtered, the nucleophile (0.72 mmol) was added to the solution and left to stir for 5 minutes, after which $CoCl_2$ was added, slowly. The solution initially turned dark blue on addition, but after being left to stir overnight, a dark red solution evolved. The solution was filtered, and the solvent removed *in vacuo*.

4a (0.32 g, 0.39 mmol, 54 %): *m/z* (LSI^+): 703 (100 %, $[L^1Co_2Cl]^+$). Anal. Calc. for $C_{38}H_{60}Cl_2Co_2N_6O_2$: C, 55.54; H, 7.36; N, 10.23. Found: C, 55.68; H, 7.50; N, 10.05.

4b (0.47 g, 0.54 mmol, 75 %): *m/z* (LSI^+): 703 (100 %, $[L^1Co_2Cl]^+$). Anal. Calc. for $C_{41}H_{64}Cl_2Co_2N_6O_2$: C, 57.15; H, 7.49; N, 9.75. Found: C, 57.19; H, 7.59; N, 9.63. UV-Vis λ_{max}/nm (ε/$dm^3mol^{-1}cm^{-1}$): 473 (95.7), 538 (82.4).

4c (0.42 g, 0.53 mmol, 70 %): *m/z* (LSI^+): 703 (100 %, $[L^1Co_2Cl]^+$). Anal. Calc. for $C_{39}H_{59}Cl_2Co_2N_5O_2$: C, 57.22; H, 7.26; N, 8.55. Found: C, 57.12; H, 7.26; N, 8.46. UV-Vis λ_{max}/nm (ε/$dm^3mol^{-1}cm^{-1}$): 474 (95.9), 509 (78.9), 535 (76.3).

Copolymerization Conditions

Cyclohexene oxide (2.5 mL, 25 mmol) and the catalyst (0.025 mmol) were added to a Schlenk tube. The cyclohexene oxide was de-gassed, before being left stirring under 1 atm CO_2, at 80 °C, for a certain number of hours. The crude reaction mixture was then taken up in CH_2Cl_2 and a 0.2 mL of a 5% solution of HCl/MeOH was added. The solution was evaporated in air, after which the product was dried, *in vacuo,* overnight. No further purification of the polymer was undertaken as the vacuum was sufficient to remove unreacted cyclohexene oxide.

Turn-over-number was calculated as [(isolated yield – weight catalyst)/142.1]/moles catalyst.

Kinetic Studies

Experiments to determine the influence of [catalyst]

A three-necked round bottom flask was dried overnight at 140 °C, fitted with the *in-situ* IR probe, a stopper and evacuated for 30 minutes. Separately, a Schlenk tube was loaded with **4a**

(2.43, 4.87, 9.74, 12.2 and 14.6 mM) and cyclohexene oxide (2.5 mL, 25 mmol). The solution was transferred into the round bottom flask under CO_2 and the flask heated to 80 °C. The IR probe was initiated, and scans were taken every minute over the reaction period until the rate began to decrease due to viscosity. The initial rates were determined as the slope of the linear regions of plots of absorption versus time for each concentration of catalyst (Figure S20).

***Experiments to determine the influence of* [CHO]$_0$**

A three-necked round bottom flask was dried overnight at 140 °C, fitted with the *in-situ* IR probe, a stopper and evacuated for 30 minutes. Separately, a Schlenk tube was loaded with **3a** (15 mg, 0.018 mmol), cyclohexene oxide ((3 – x) mL) and diethylcarbonate (x mL; x = 0.5, 1, 1.5, 2 or 2.5). The solution was transferred into the round bottom flask under CO_2 and the flask heated to 80 °C. A single 256 scan background spectrum was collected after addition of the solution to eliminate the absorption at 1750 cm^{-1} arising from diethylcarbonate, which overlaps with the carbonyl resonance of the growing chain. Scans were taken every minute over the reaction period until the rate began to decrease due to viscosity. The initial rates were determined as the slope of the linear regions of the plots of absorption versus time for each concentration of CHO (Figures S21-22).

X-ray Crystallographic Data

Data	**1a**	**1b**	**2a**
formula	$C_{34}H_{54}Co_3I_4N_4O_2$	$C_{34}H_{54}Br_4Co_3N_4O_2$	$C_{68}H_{108}Cl_5Co_4KN_8O_4$
solvent	$3C_4H_8O$	$3C_4H_8O$	$7.5CH_2Cl_2$
fw	1451.51	1263.55	2190.64
T (°C)	–100	–100	–100
space group	*P*2$_1$/*c* (no. 14)	*P*2$_1$/*c* (no. 14)	*Pnma* (no. 62)
a (Å)	11.79263(10)	11.69346(15)	23.2374(5)
b (Å)	21.62584(18)	20.8757(3)	30.6555(6)
c (Å)	22.16086(19)	22.0206(2)	14.1318(4)
α (deg)	—	—	—
β (deg)	102.5923(9)	102.0342(12)	—
γ (deg)	—	—	—
V (Å^3)	5515.64(8)	5257.30(11)	10066.8(4)
Z	4	4	4 [a]
ρ_{calcd} (g cm^{-3})	1.748	1.596	1.445
λ (Å)	0.71073	0.71073	0.71073
μ (mm^{-1})	3.174	4.021	1.267
R_1(obs) [b]	0.0246	0.0323	0.0572
wR_2(all) [c]	0.0548	0.0702	0.1437

data	**2b**	**3a**	**3b**
formula	$C_{68}H_{108}Cl_5Co_4KN_8O_4$	$[C_{34}H_{54}Cl_3Co_2N_4O_2]($ $C_6H_{16}N)$	$[C_{34}H_{54}Cl_3Co_2N_4O_2]($ $C_9H_{17}N_2)$
solvent	$8CH_2Cl_2$	$2CH_2Cl_2$	$C_4H_8O{\cdot}0.5C_6H_{14}$
fw	2233.10	1047.07	1043.46
T (°C)	–100	–100	–100
space group	$P2_1/c$ (no. 14)	$P2_1/n$ (no. 14)	$P\bar{1}$ (no. 2)
a (Å)	11.78965(15)	14.4425(2)	12.4636(4)
b (Å)	31.1301(4)	21.5810(3)	15.6121(6)
c (Å)	27.4398(3)	16.8129(2)	15.8197(5)
α (deg)	—	—	69.978(3)
β (deg)	96.1289(13)	105.0867(14)	71.369(3)
γ (deg)	—	—	85.244(3)
V (Å^3)	10013.2(2)	5059.69(12)	2739.42(18)
Z	4	4	2
ρ_{calcd} (g cm^{-3})	1.481	1.375	1.265
λ (Å)	1.54184	0.71073	0.71073
μ (mm^{-1})	11.008	1.064	0.796
R_1(obs) [b]	0.0803	0.0322	0.0353
wR_2(all) [c]	0.2113	0.0844	0.0918

data	**3c**	**4a**	**4b**
formula	$[C_{34}H_{54}Cl_3Co_2N_4O_2]($ $C_8H_{16}N_3)$	$C_{38}H_{60}Cl_2Co_2N_6O_2$	$C_{41}H_{64}Cl_2Co_2N_6O_2$
solvent	—	$2C_4H_8O$	$4.5CH_2Cl_2$
fw	929.26	965.89	1243.91
T (°C)	–100	–100	–100
space group	$P2_1/n$ (no. 14)	$P\bar{1}$ (no. 2)	$C2/c$ (no. 15)
a (Å)	15.0900(2)	11.3806(4)	35.3728(13)
b (Å)	20.2875(3)	13.8405(4)	20.4934(4)
c (Å)	15.7020(2)	15.7508(6)	19.9836(6)
α (deg)	—	96.278(3)	—
β (deg)	104.0816(15)	96.347(3)	124.046(5)
γ (deg)	—	91.870(3)	—

V (Å^3)	4662.54(11)	2448.46(14)	12003.2(9)
Z	4	2	8
ρ_{calcd} (g cm^{-3})	1.324	1.310	1.377
λ (Å)	1.54184	1.54184	0.71073
μ (mm^{-1})	7.478	6.675	1.082
R_1(obs) [b]	0.0388	0.0593	0.0434
wR_2(all) [c]	0.1072	0.1654	0.1319

[a] The molecule has crystallographic C_S symmetry. [b] $R_1 = \Sigma||F_o| - |F_c||/ \Sigma|F_o|$. [c] $wR_2 = \{ \Sigma[w(F_o^2 - F_c^2)^2] / \Sigma[w(F_o^2)^2]\}^{1/2}$; $w^{-1} = \sigma^2(F_o^2) + (aP)^2 + bP$.

Table S1. Crystallographic Data for compounds **1a**, **1b**, **2a**, **2b**, **3a**, **3b**, **3c**, **4a** and **4b**.

Table S1 provides a summary of the crystallographic data for compounds **1a**, **1b**, **2a**, **2b**, **3a**, **3b**, **3c**, **4a** and **4b**. Data were collected using Oxford Diffraction Xcalibur 3 (**1a**, **1b**, **2a**, **3a**, **3b** and **4b**) and Xcalibur PX Ultra (**2b**, **3c** and **4a**) diffractometers, and the structures were refined based on F^2 using the SHELXTL and SHELX-97 program systems.[2] CCDC 825190 to 825198.

The X-ray crystal structure of 1a

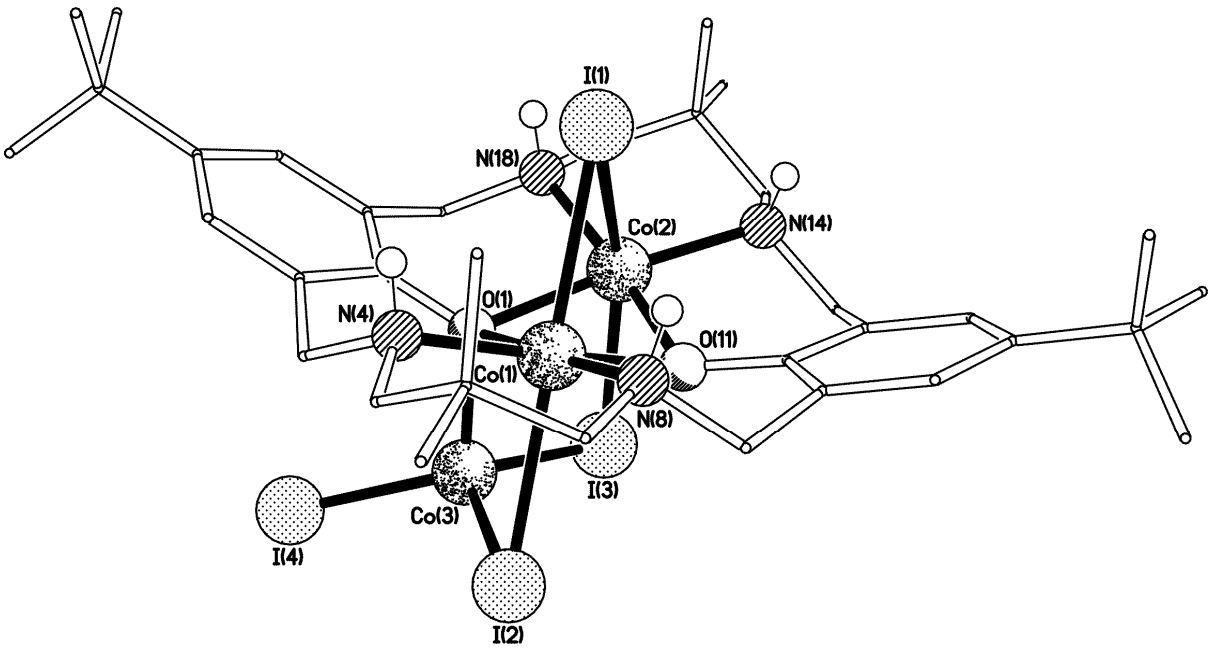

Fig. S1 The molecular structure of **1a**.

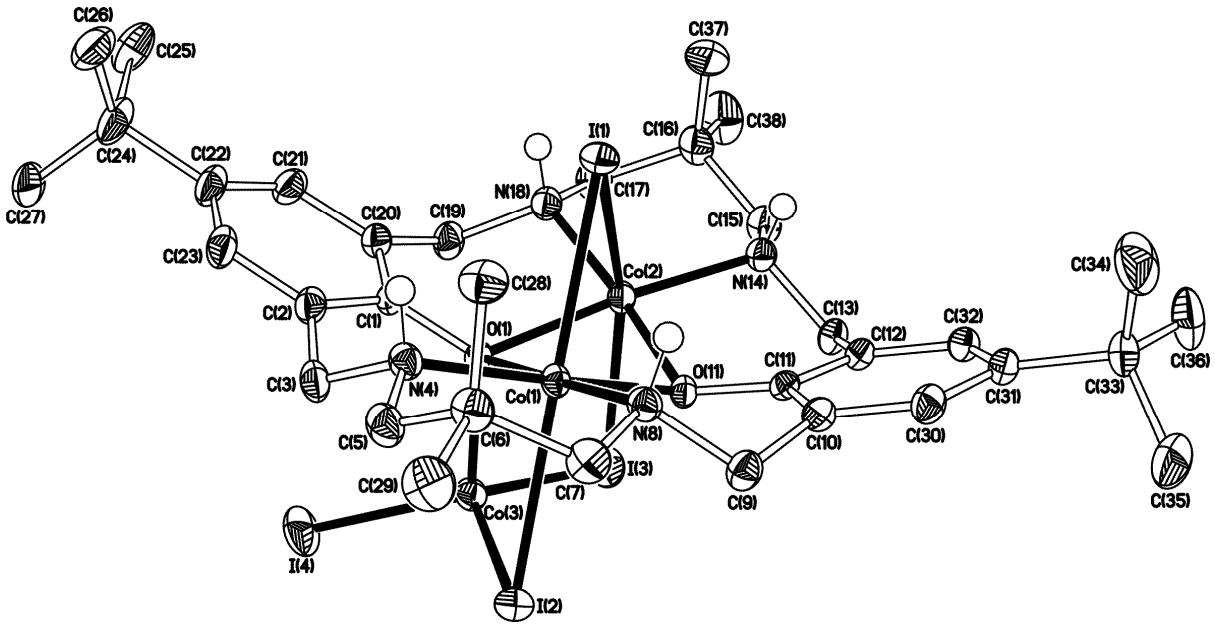

Fig. S2 The molecular structure of **1a** (50% probability ellipsoids).

The structures of **1a** and its isomorphous bromide counterpart **1b** are similar to the previously reported acetate analogue[3] but with a noticeably flatter dished conformation, the $C_{(t\text{-Bu})}\cdots C_{(t\text{-Bu})}$ separation being *ca*. 13.57 Å in both **1a** and **1b**, *cf*. *ca*. 12.42 Å in the acetate species. The distances between the metal atoms and the macrocyclic ligand show the same pattern in all three structures but are consistently slightly shorter in the halogen species (see Table S2). The coordination to the bridging halide X(1) in **1a** and **1b** is asymmetric with the bond to Co(2) being *ca*. 0.10 Å longer than that to Co(1). This asymmetry is also seen in the Co–X bonds *trans* to the bonds to the bridging halide such that the Co(2)–X(3) bond is *ca*. 0.05 Å longer than its Co(1)–X(2) counterpart. Despite this asymmetry in the Co–X bonds around Co(1) and Co(2), however, the bonds between Co(3) and X(2) and X(3) are symmetric.

The I(4) iodine atom in the structure of **1a** was found to be disordered. Two sites of *ca*. 97 and 3% occupancy were identified, the respective Co–I distances were restrained to be similar, and the major occupancy iodine atom was refined anisotropically whilst the minor occupancy iodine atom was refined isotropically. The C(24)-based *t*-butyl group was found to be disordered. Two orientations of *ca*. 78 and 22% occupancy were identified, their geometries optimised, and only the non-hydrogen atoms of the major occupancy orientation were refined anisotropically (those of the minor occupancy orientation were refined isotropically). Two of the three included tetrahydrofuran solvent molecules were found to be

disordered. Three orientations of *ca*. 43:32:25 and 40:37:23% occupancy were identified for the O(50) and O(60)-based molecules respectively. The geometries of all six orientations were optimised, the thermal parameters of adjacent atoms were restrained to be similar, and all of the atoms were refined isotropically. All four N–H protons were located from Δ*F* maps and refined freely subject to an N–H distance constraint of 0.90 Å.

The X-ray crystal structure of 1b

The C(24)-based *t*-butyl group in the structure of **1b** was found to be disordered. Two orientations of *ca*. 95 and 5% occupancy were identified, their geometries optimised, the thermal parameters of adjacent atoms restrained to be similar, and only the non-hydrogen atoms of the major occupancy orientation were refined anisotropically (those of the minor occupancy orientation were refined isotropically). Two of the three included tetrahydrofuran solvent molecules were found to be disordered. Three orientations of *ca*. 45:35:20 and 47:29:24% occupancy were identified for the O(50) and O(60)-based molecules respectively. The geometries of all six orientations were optimised, the thermal parameters of adjacent atoms were restrained to be similar, and all of the atoms were refined isotropically. All four N–H protons were located from Δ*F* maps and refined freely subject to an N–H distance constraint of 0.90 Å.

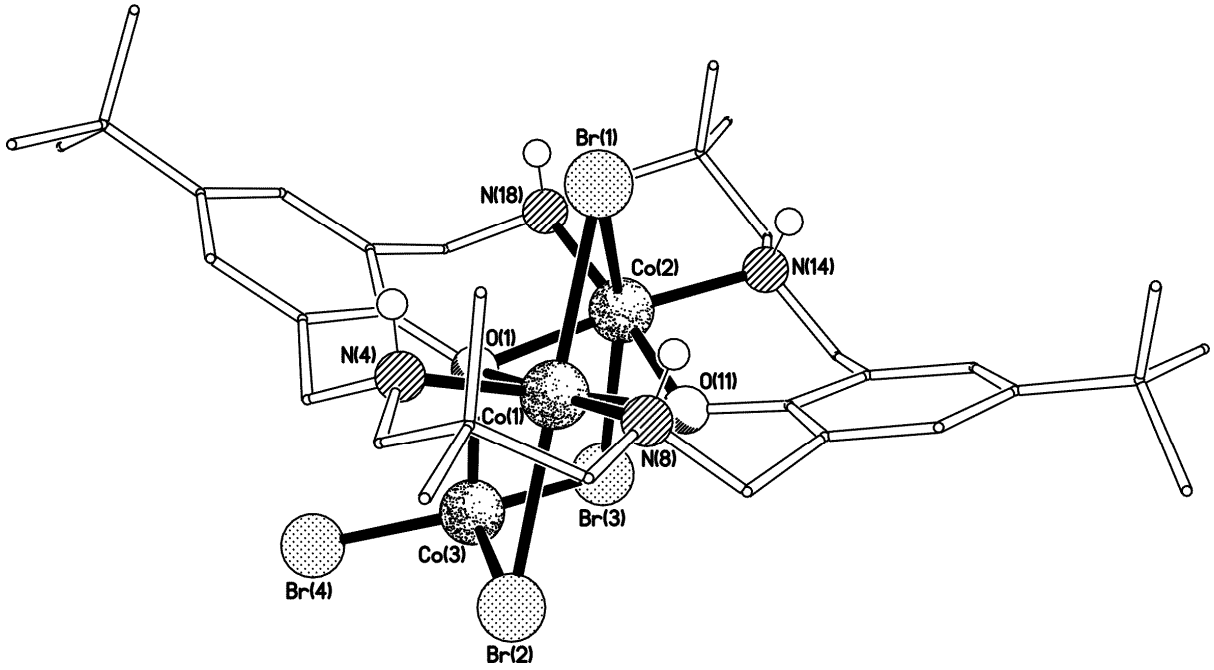

Fig. S3 The molecular structure of **1b**.

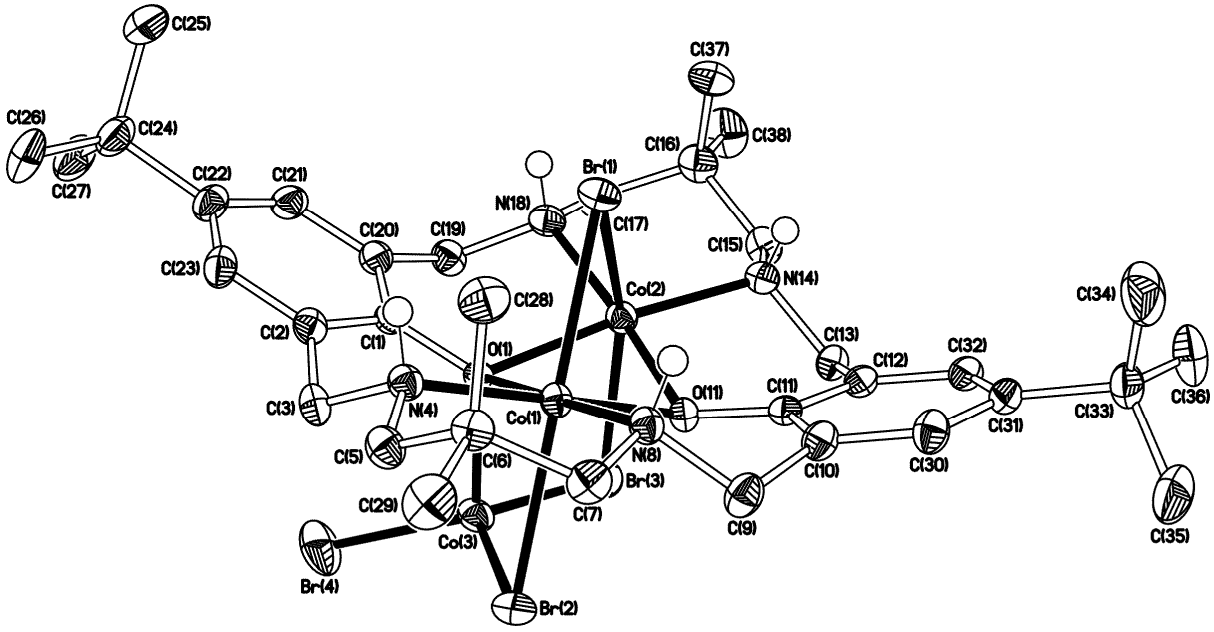

Fig. S4 The molecular structure of **1b** (50% probability ellipsoids).

	1a [X = I]	**1b** [X = Br]		**1a** [X = I]	**1b** [X = Br]
Co(1)–X(1)	2.8916(3)	2.6704(4)	Co(1)–X(2)	2.9333(3)	2.7438(4)
Co(1)–O(1)	2.1945(13)	2.1844(14)	Co(1)–N(4)	2.1114(16)	2.1091(18)
Co(1)–N(8)	2.0925(17)	2.0986(18)	Co(1)–O(11)	2.0494(13)	2.0471(14)
Co(2)–X(1)	2.9774(3)	2.7767(4)	Co(2)–X(3)	2.9944(3)	2.7860(4)
Co(2)–O(1)	2.1773(13)	2.1538(14)	Co(2)–O(11)	2.0497(13)	2.0494(14)
Co(2)–N(14)	2.1080(17)	2.1064(18)	Co(2)–N(18)	2.1072(17)	2.1085(18)
Co(3)–X(2)	2.6046(3)	2.4291(4)	Co(3)–X(3)	2.5996(3)	2.4240(4)
Co(3)–X(4)	2.5429(3)	2.3521(4)	Co(3)–X(4')	2.575(8)	n/a
Co(3)–O(1)	2.0049(12)	2.0109(14)	Co(1)···Co(2)	2.9822(4)	2.9490(4)
Co(1)···Co(3)	3.2910(4)	3.2575(4)	Co(2)···Co(3)	3.3240(4)	3.2739(4)
X(1)–Co(1)–X(2)	165.654(11)	162.059(14)	X(1)–Co(1)–O(1)	83.23(3)	81.82(4)
X(1)–Co(1)–N(4)	95.12(5)	97.32(5)	X(1)–Co(1)–N(8)	95.56(4)	97.34(5)
X(1)–Co(1)–O(11)	82.58(4)	82.27(4)	X(2)–Co(1)–O(1)	84.46(3)	82.68(4)
X(2)–Co(1)–N(4)	92.15(4)	91.60(5)	X(2)–Co(1)–N(8)	96.35(4)	97.67(5)
X(2)–Co(1)–O(11)	88.58(4)	86.91(4)	O(1)–Co(1)–N(4)	89.67(6)	89.85(6)
O(1)–Co(1)–N(8)	176.93(6)	176.89(6)	O(1)–Co(1)–O(11)	82.76(5)	82.87(5)
N(4)–Co(1)–N(8)	93.25(6)	93.22(7)	N(4)–Co(1)–O(11)	172.29(6)	172.70(6)
N(8)–Co(1)–O(11)	94.30(6)	94.06(6)	X(1)–Co(2)–X(3)	161.460(11)	158.027(14)
X(1)–Co(2)–O(1)	81.47(3)	79.86(4)	X(1)–Co(2)–O(11)	80.40(3)	79.58(4)
X(1)–Co(2)–N(14)	100.71(4)	103.26(5)	X(1)–Co(2)–N(18)	94.21(5)	95.35(5)
X(3)–Co(2)–O(1)	82.42(3)	81.16(4)	X(3)–Co(2)–O(11)	88.65(3)	87.41(4)
X(3)–Co(2)–N(14)	94.63(4)	94.76(5)	X(3)–Co(2)–N(18)	95.05(5)	95.79(5)
O(1)–Co(2)–O(11)	83.18(5)	83.58(5)	O(1)–Co(2)–N(14)	174.83(6)	174.12(7)
O(1)–Co(2)–N(18)	90.56(6)	90.51(6)	O(11)–Co(2)–N(14)	92.53(6)	92.04(6)
O(11)–Co(2)–N(18)	172.27(6)	172.79(7)	N(14)–Co(2)–N(18)	93.94(7)	94.13(7)
X(2)–Co(3)–X(3)	118.217(11)	120.870(15)	X(2)–Co(3)–X(4)	112.86(2)	115.536(15)
X(2)–Co(3)–X(4')	123.7(4)	n/a	X(2)–Co(3)–O(1)	97.56(4)	94.86(4)
X(3)–Co(3)–X(4)	116.26(2)	115.477(15)	X(3)–Co(3)–X(4')	105.9(4)	n/a
X(3)–Co(3)–O(1)	96.66(4)	93.75(4)	X(4)–Co(3)–O(1)	111.99(4)	110.47(4)
X(4')–Co(3)–O(1)	110.84(18)	n/a	Co(1)–X(1)–Co(2)	61.058(8)	65.522(10)

Co(1)–X(2)–Co(3)	72.646(8)	77.795(11)	Co(2)–X(3)–Co(3)	72.525(8)	77.516(11)

Table S2. Selected bond lengths (Å) and angles (°) for **1a** and **1b**.

	1a [X = I]	**1b** [X = Br]	**Ac**
M(1)–O(1)	2.1945(13)	2.1844(14)	2.2273(17)
M(1)–N(4)	2.1114(16)	2.1091(18)	2.133(2)
M(1)–N(8)	2.0925(17)	2.0986(18)	2.112(2)
M(1)–O(11)	2.0494(13)	2.0471(14)	2.0571(16)
M(2)–O(1)	2.1773(13)	2.1538(14)	2.1897(16)
M(2)–O(11)	2.0497(13)	2.0494(14)	2.0845(17)
M(2)–N(14)	2.1080(17)	2.1064(18)	2.138(2)
M(2)–N(18)	2.1072(17)	2.1085(18)	2.139(2)
M(3)–O(1)	2.0049(12)	2.0109(14)	2.0075(15)
M(1)···M(2)	2.9822(4)	2.9490(4)	3.0607(4)

Table S3. Selected bond lengths (Å) for **1a**, **1b** and the analogous acetate complex (**Ac**)[3].

The X-ray crystal structure of 2a

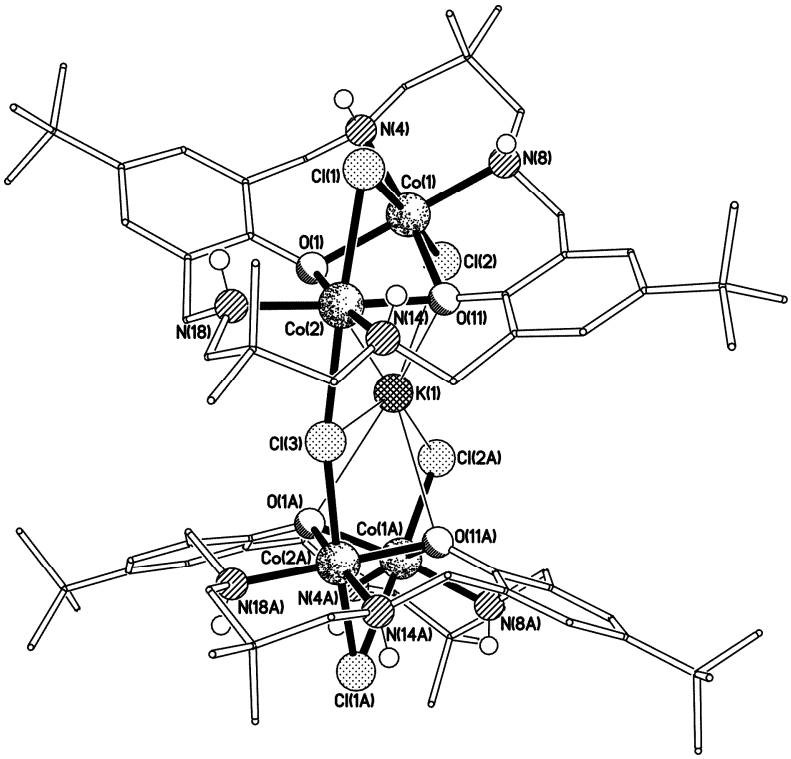

Fig. S5 The molecular structure of the C_S symmetric complex **2a**.

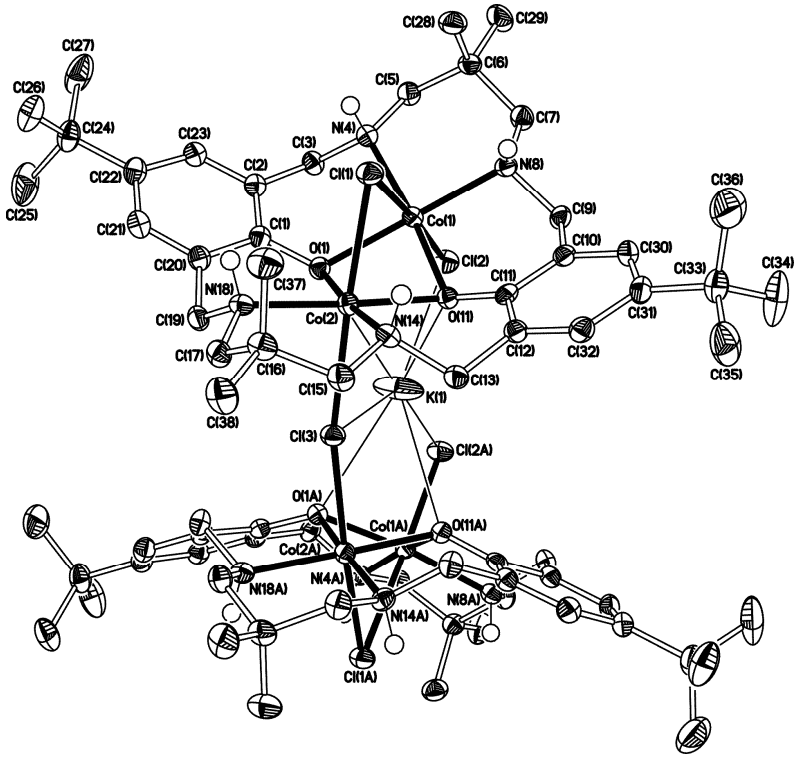

Fig. S6 The molecular structure of the C_S symmetric complex **2a** (50% probability ellipsoids).

The structure of **2a** has C_S symmetry about a plane that passes through K(1) and the bridging chloride Cl(3), and bisects the Co(2)–Cl(3)–Co(2A) angle. The unique $[L^1Co_2Cl_3]$ unit has the usual dished conformation with a $C_{(t\text{-Bu})}\cdots C_{(t\text{-Bu})}$ separation of *ca*. 13.65 Å. The coordination to the bridging chloride Cl(1) is asymmetric with the bond to Co(1) being *ca*. 0.16 Å longer than that to Co(2). A corresponding asymmetry is also seen in the Co–Cl bonds *trans* to the Co–Cl(1) bonds such that the Co(2)–Cl(3) bond is *ca*. 0.22 Å longer than its Co(1)–Cl(2) counterpart, though the bridging and terminal characters of Cl(3) and Cl(2) respectively complicate the situation. The two $[L^1Co_2Cl_3]$ units are linked by the bridging chloride Cl(3) [Co(2)–Cl(3)–Co(2A) 163.60(6)°] and are arranged in a clamshell-like fashion such that their respective N_4 planes are inclined by *ca*. 45° and the Co(1)···Co(1A) separation is *ca*. 7.23 Å. The potassium atom K(1) sits in the open mouth of this clamshell, binding to the bridging chloride Cl(3), the terminal chloride Cl(2) of both Co_2Cl_3(macrocycle) units, and all four of the oxygen atoms, resulting in a mono-capped trigonal prismatic geometry coordination geometry.

The 7.5 dichloromethane solvent molecules per complex (3.75 per asymmetric unit) in the structure of **2a** were found to be distributed over 6 discrete sites. Two of these are in general positions [those based on C(40) and C(50)], with the others being adjacent to mirror planes

[those based on C(60), C(70), C(80) and C(90)]. Consideration of the thermal parameters suggested that the C(90) site was not always occupied, and the refinements worked well with an overall 50% occupancy of this site (and thus only 25% occupancy in the asymmetric unit). The C(70), C(80) and C(90)-based dichloromethane solvent molecules were all found to be disordered. In each case two orientations were identified, of *ca.* 39:11, 34:16 and 18:7% occupancy for the C(70), C(80) and C(90)-based molecules respectively. (In each case, two further orientations with the same pairs of occupancies are generated by action of the adjacent mirror plane.) The geometries of all six orientations were optimised, the thermal parameters of chemically equivalent adjacent atoms were restrained to be similar, and all of the chlorine atoms were refined anisotropically (except for those of the 7% occupancy orientation of the C(90)-based molecule); all of the carbon atoms were refined isotropically. All four N–H protons were located from Δ*F* maps and refined freely subject to an N–H distance constraint of 0.90 Å.

The X-ray crystal structure of 2b

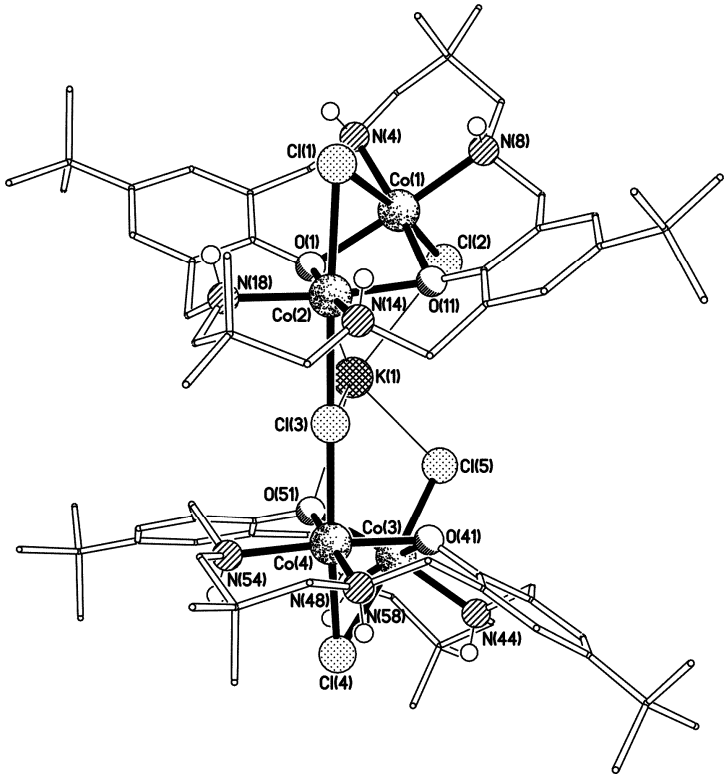

Fig. S7 The molecular structure of **2b**.

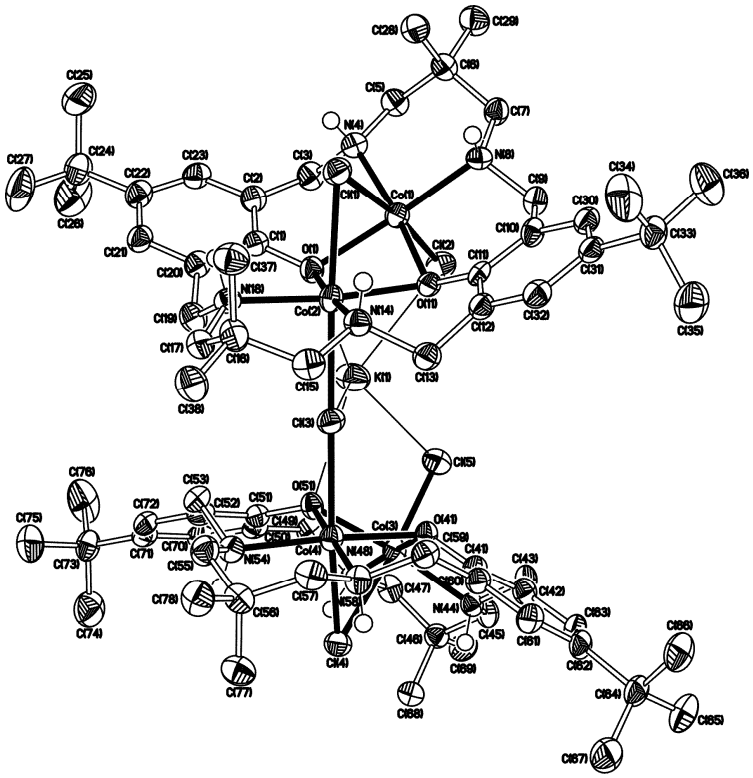

Fig. S8 The molecular structure of **2b** (50% probability ellipsoids).

The structure of **2b** is essentially as that of **2a**, but with a sightly higher degree of solvation (8 dichloromethane molecules per complex in **2b** *cf.* 7.5 in **2a**) and without the mirror plane. Both of the $[L^1Co_2Cl_3]$ units have the usual dished conformation with $C_{(t\text{-}Bu)}\cdots C_{(t\text{-}Bu)}$ separations of *ca*. 13.65 and 13.60 Å for the Co(1)/Co(2) and Co(3)/Co(4) units respectively. The coordination to the bridging chlorides Cl(1) and Cl(4) are asymmetric with the Co(1)–Cl(1) and Co(3)–Cl(4) bonds *ca*. 0.14 and 0.09 Å longer than the Co(2)–Cl(1) and Co(4)–Cl(4) bonds respectively. A corresponding asymmetry is also seen in the Co–Cl bonds *trans* to the Co–Cl(1) bonds such that the Co(2)–Cl(3) and Co(4)–Cl(3) bonds are *ca*. 0.20Å longer than their Co(1)–Cl(2) and Co(3)–Cl(5) counterparts, though the bridging and terminal characters of Cl(3) and Cl(2)/Cl(5) respectively complicate the situation. The two $[L^1Co_2Cl_3]$ units are linked by the bridging chloride Cl(3) [Co(2)–Cl(3)–Co(4) 175.75(7)°] and are arranged in a clamshell-like fashion such that their respective N_4 planes are inclined by *ca*. 50° and the Co(1)···Co(3) separation is *ca*. 7.51 Å. The corresponding values in **2a** were 45° and 7.23 Å, so it is clear that the "mouth" of the clamshell opens wider in **2b**. This wider opening results in a different coordination around the potassium atom, with here the potassium linking to only one of the oxygen atoms in each macrocycle rather than both as

seen in **2a**. (In **2a**, the K–O separations are 3.135(3) and 3.077(3) Å to O(1) and O(11) respectively, whereas in **2b** they are 2.918(5), 2.922(4), 3.937(4) and 3.940(4) Å to O(1), O(51), O(11) and O(41) respectively.) As in **2a**, the potassium atom also binds to the bridging chloride Cl(3) and the terminal chlorides of both [$L^1Co_2Cl_3$] units [Cl(2) and Cl(5)]. The result is a five-coordinate geometry with a whole hemisphere around the potassium centre "empty", and this site is occupied by the disordered dichloromethane solvent molecule (see below) with one of the partial occupancy chlorine atoms approaching at a distance of *ca*. 2.89 Å.

Only one of the eight dichloromethane molecules in the structure of **2b** was found to be disordered [that based on C(80)], and for this molecule three orientations of *ca*. 67:19:14% occupancy were identified. The geometries of the three orientations were optimised, the thermal parameters of chemically equivalent adjacent atoms were restrained to be similar, and only the non-hydrogen atoms of the major occupancy orientation were refined anisotropically (the remainder were refined isotropically). The eight N–H protons could not all be reliably located and so they were placed in idealised positions and refined using a riding model with an N–H distance 0.90 Å.

Co(1)–Cl(1)	2.7155(10)	Co(1)–Cl(2)	2.4132(10)
Co(1)–O(1)	2.115(3)	Co(1)–N(4)	2.117(3)
Co(1)–N(8)	2.111(3)	Co(1)–O(11)	2.123(2)
Co(2)–Cl(1)	2.5554(10)	Co(2)–Cl(3)	2.6381(5)
Co(2)–O(1)	2.102(2)	Co(2)–O(11)	2.092(2)
Co(2)–N(14)	2.119(3)	Co(2)–N(18)	2.110(3)
Cl(2)–K(1)	2.9823(14)	Cl(3)–K(1)	2.9420(19)
O(1)–K(1)	3.135(3)	O(11)–K(1)	3.077(3)
Co(1)–Co(2)	2.9490(7)		
Cl(1)–Co(1)–Cl(2)	175.41(4)	Cl(1)–Co(1)–O(1)	78.63(7)
Cl(1)–Co(1)–N(4)	91.79(8)	Cl(1)–Co(1)–N(8)	91.81(9)
Cl(1)–Co(1)–O(11)	77.69(7)	Cl(2)–Co(1)–O(1)	98.20(7)
Cl(2)–Co(1)–N(4)	91.65(8)	Cl(2)–Co(1)–N(8)	91.07(9)
Cl(2)–Co(1)–O(11)	98.68(7)	O(1)–Co(1)–N(4)	92.08(11)
O(1)–Co(1)–N(8)	169.46(11)	O(1)–Co(1)–O(11)	82.49(9)
N(4)–Co(1)–N(8)	92.64(12)	N(4)–Co(1)–O(11)	168.91(11)
N(8)–Co(1)–O(11)	91.21(11)	Cl(1)–Co(2)–Cl(3)	176.05(4)
Cl(1)–Co(2)–O(1)	82.69(7)	Cl(1)–Co(2)–O(11)	82.03(7)
Cl(1)–Co(2)–N(14)	93.08(9)	Cl(1)–Co(2)–N(18)	96.07(8)
Cl(3)–Co(2)–O(1)	95.51(7)	Cl(3)–Co(2)–O(11)	94.29(7)
Cl(3)–Co(2)–N(14)	88.45(9)	Cl(3)–Co(2)–N(18)	87.49(9)
O(1)–Co(2)–O(1)	83.55(9)	O(1)–Co(2)–N(14)	174.13(11)
O(1)–Co(2)–N(18)	91.69(11)	O(11)–Co(2)–N(14)	91.85(11)
O(11)–Co(2)–N(18)	175.05(11)	N(14)–Co(2)–N(18)	92.82(12)
Co(1)–Cl(1)–Co(2)	67.96(3)	Co(1)–Cl(2)–K(1)	83.64(3)

Co(2)–Cl(3)–	163.60(6)	Co(2)–Cl(3)–K(1)	82.19(3)

Table S4. Selected bond lengths (Å) and angles (°) for **2a**.

Co(1)–Cl(1)	2.7179(18)	Co(1)–Cl(2)	2.3903(18)
Co(1)–O(1)	2.118(4)	Co(1)–N(4)	2.113(5)
Co(1)–N(8)	2.113(5)	Co(1)–O(11)	2.114(4)
Co(2)–Cl(1)	2.5799(18)	Co(2)–Cl(3)	2.5948(18)
Co(2)–O(1)	2.110(4)	Co(2)–O(11)	2.077(4)
Co(2)–N(14)	2.134(5)	Co(2)–N(18)	2.122(5)
Co(3)–Cl(4)	2.6828(18)	Co(3)–Cl(5)	2.3848(18)
Co(3)–O(41)	2.111(4)	Co(3)–N(44)	2.119(5)
Co(3)–N(48)	2.105(5)	Co(3)–O(51)	2.130(4)
Co(4)–Cl(3)	2.5828(18)	Co(4)–Cl(4)	2.5900(18)
Co(4)–O(41)	2.083(4)	Co(4)–O(51)	2.105(4)
Co(4)–N(54)	2.120(5)	Co(4)–N(58)	2.110(5)
Cl(2)–K(1)	3.100(2)	Cl(3)–K(1)	3.097(2)
Cl(5)–K(1)	3.089(2)	O(1)–K(1)	2.918(5)
O(51)–K(1)	2.922(4)	Co(1)···Co(2)	2.9358(14)
Co(3)···Co(4)	2.9325(14)		

Cl(1)–Co(1)–Cl(2)	172.11(7)	Cl(1)–Co(1)–O(1)	78.09(12)
Cl(1)–Co(1)–N(4)	91.84(14)	Cl(1)–Co(1)–N(8)	91.23(14)
Cl(1)–Co(1)–O(11)	77.57(12)	Cl(2)–Co(1)–O(1)	95.81(13)
Cl(2)–Co(1)–N(4)	93.30(14)	Cl(2)–Co(1)–N(8)	94.53(14)
Cl(2)–Co(1)–O(11)	96.96(12)	O(1)–Co(1)–N(4)	91.28(18)
O(1)–Co(1)–N(8)	168.78(18)	O(1)–Co(1)–O(11)	83.95(16)
N(4)–Co(1)–N(8)	92.48(19)	N(4)–Co(1)–O(11)	169.06(18)
N(8)–Co(1)–O(11)	90.48(17)	Cl(1)–Co(2)–Cl(3)	173.74(6)
Cl(1)–Co(2)–O(1)	81.49(12)	Cl(1)–Co(2)–O(11)	81.48(12)
Cl(1)–Co(2)–N(14)	94.61(15)	Cl(1)–Co(2)–N(18)	92.35(14)
Cl(3)–Co(2)–O(1)	93.47(12)	Cl(3)–Co(2)–O(11)	94.45(12)
Cl(3)–Co(2)–N(14)	90.24(15)	Cl(3)–Co(2)–N(18)	91.43(14)
O(1)–Co(2)–O(11)	85.06(15)	O(1)–Co(2)–N(14)	175.29(18)
O(1)–Co(2)–N(18)	90.94(17)	O(11)–Co(2)–N(14)	91.76(17)
O(11)–Co(2)–N(18)	173.08(18)	N(14)–Co(2)–N(18)	91.87(19)
Cl(4)–Co(3)–Cl(5)	172.18(7)	Cl(4)–Co(3)–O(41)	78.23(11)
Cl(4)–Co(3)–N(44)	92.22(14)	Cl(4)–Co(3)–N(48)	90.80(14)
Cl(4)–Co(3)–O(51)	78.52(12)	Cl(5)–Co(3)–O(41)	96.75(12)
Cl(5)–Co(3)–N(44)	93.89(14)	Cl(5)–Co(3)–N(48)	93.85(15)
Cl(5)–Co(3)–O(51)	95.08(12)	O(41)–Co(3)–N(44)	91.12(17)
O(41)–Co(3)–N(48)	168.66(18)	O(41)–Co(3)–O(51)	83.97(15)
N(44)–Co(3)–N(48)	92.18(19)	N(44)–Co(3)–O(51)	170.22(18)
N(48)–Co(3)–O(51)	91.10(18)	Cl(3)–Co(4)–Cl(4)	173.20(6)
Cl(3)–Co(4)–O(41)	94.69(12)	Cl(3)–Co(4)–O(51)	93.37(12)
Cl(3)–Co(4)–N(54)	91.41(15)	Cl(3)–Co(4)–N(58)	91.58(15)
Cl(4)–Co(4)–O(41)	80.92(12)	Cl(4)–Co(4)–O(51)	81.15(12)
Cl(4)–Co(4)–N(54)	92.69(15)	Cl(4)–Co(4)–N(58)	93.69(15)
O(41)–Co(4)–O(51)	85.29(15)	O(41)–Co(4)–N(54)	173.01(18)
O(41)–Co(4)–N(58)	91.15(17)	O(51)–Co(4)–N(54)	90.97(18)
O(51)–Co(4)–N(58)	174.12(19)	N(54)–Co(4)–N(58)	92.08(19)
Co(1)–Cl(1)–Co(2)	67.25(5)	Co(1)–Cl(2)–K(1)	89.96(6)
Co(2)–Cl(3)–Co(4)	175.75(7)	Co(2)–Cl(3)–K(1)	87.77(6)
Co(4)–Cl(3)–K(1)	87.99(6)	Co(3)–Cl(4)–Co(4)	67.55(5)
Co(3)–Cl(5)–K(1)	90.71(6)		

Table S5. Selected bond lengths (Å) and angles (°) for **2b**.

The X-ray crystal structure of 3a

All five N–H protons were located from Δ*F* maps and refined freely subject to an N–H distance constraint of 0.90 Å.

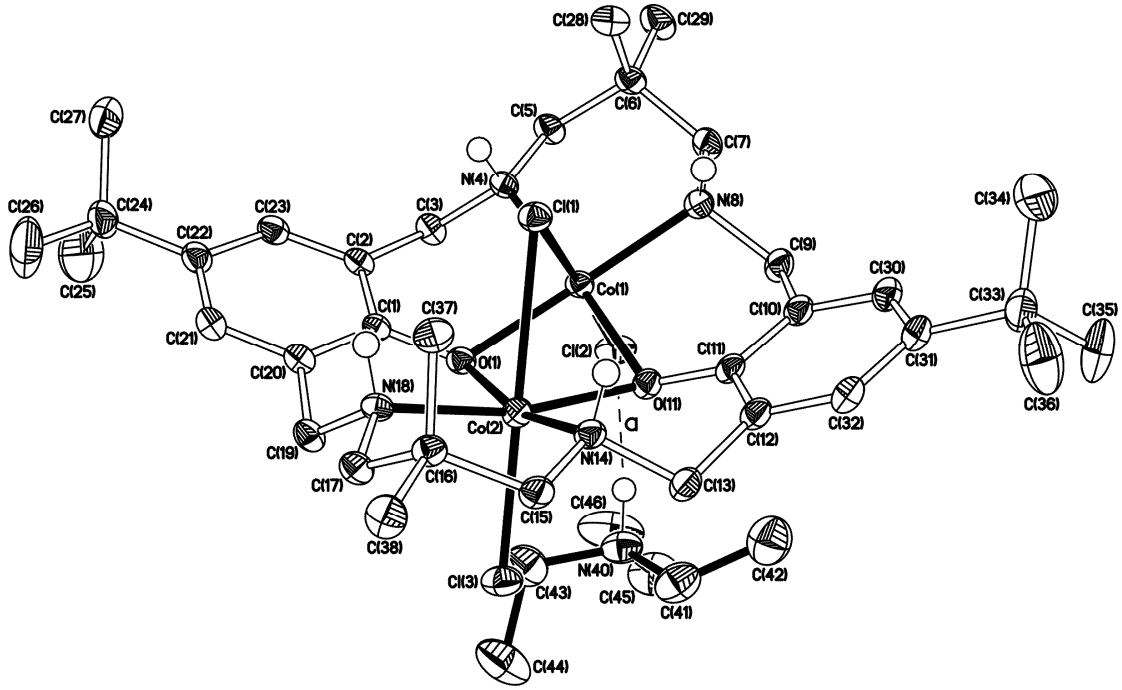

Fig. S9 The molecular structure of **3a** (50% probability ellipsoids). The N–H···Cl hydrogen bond (**a**) has N···Cl and H···Cl separations of 3.0623(13) and 2.17 Å respectively, and an N–H···Cl angle of 174°.

The X-ray crystal structure of 3b

Both the C(24) and C(33)-based *t*-butyl groups in the structure of **3b** were found to be disordered. In each case two orientations were identified, of *ca*. 90:10 and 78:22% occupancy respectively. The geometries of all four orientations were optimised, the thermal parameters of adjacent atoms restrained to be similar, and only the non-hydrogen atoms of the major occupancy orientations were refined anisotropically (those of the minor occupancy orientations were refined isotropically). The included tetrahydrofuran and hexane solvent molecules were both found to be disordered. For the tetrahydrofuran molecule, four orientations of *ca*. 31, 25, 23 and 21% occupancy were identified, their geometries were optimised, the thermal parameters of adjacent atoms were restrained to be similar, and all of the atoms were refined isotropically. The hexane molecule sits near to a centre of symmetry, and two unique orientations of *ca*. 36 and 14% occupancy were identified (two further orientations of the same pair of occupancies are generated by the operation of the inversion centre). The geometries of the two orientations were optimised, the thermal parameters of adjacent atoms were restrained to be similar, and all of the atoms were refined isotropically.

All five N–H protons were located from Δ*F* maps and refined freely subject to an N–H distance constraint of 0.90 Å.

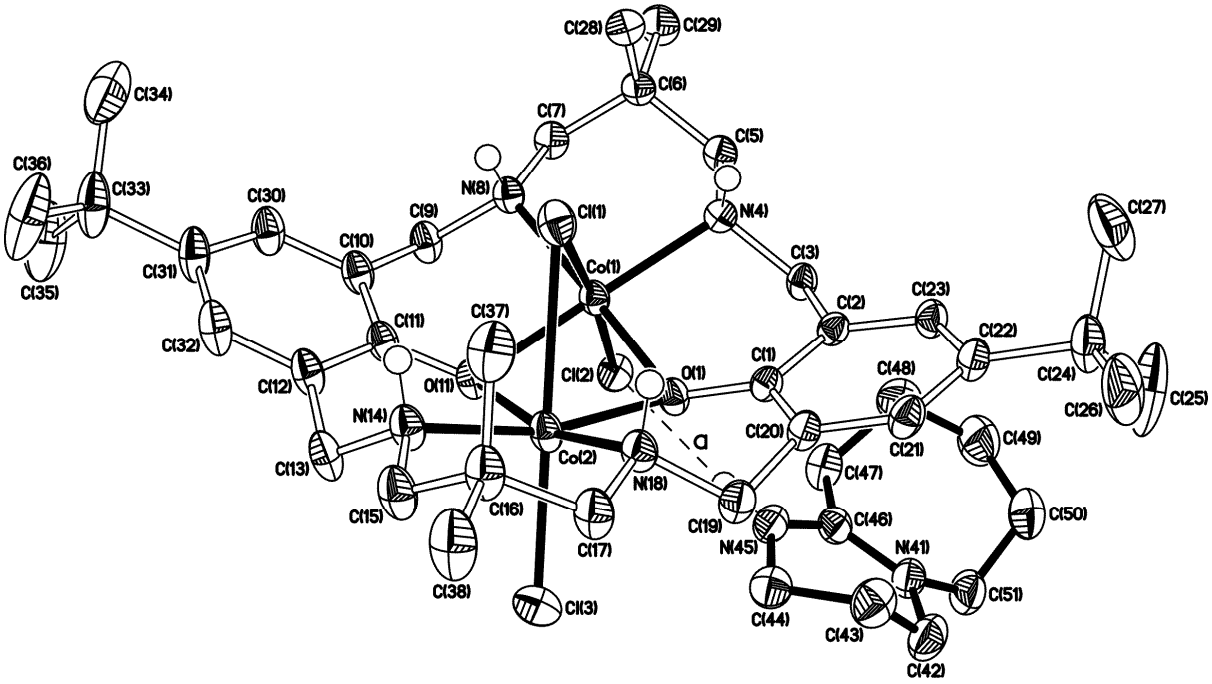

Fig. S10 The molecular structure of **3b** (50% probability ellipsoids). The N–H···Cl hydrogen bond (**a**) has N···Cl and H···Cl separations of 3.2311(14) and 2.33 Å respectively, and an N–H···Cl angle of 175°.

The X-ray crystal structure of 3c

Both the C(24) and C(33)-based *t*-butyl groups in the structure of **3c** were found to be disordered. In each case three orientations were identified, of *ca*. 69:24:7 and 51:25:24% occupancy respectively. The geometries of all six orientations were optimised, the thermal parameters of adjacent atoms restrained to be similar, and only the non-hydrogen atoms of the major occupancy orientations were refined anisotropically (those of the minor occupancy orientations were refined isotropically). The hydrogen atoms of the C(51) methyl group of the 7-methyl-1,5,7-triazabicyclo[4.4.0]dec-5-ene (MTBD) moiety were added in idealised tetrahedral positions and, as they are on an sp^3 centre bonded to an sp^2 centre, the group was allowed to rotate about the C–N bond to find the best fit with the electron density map (the SHELXL HFIX/AFIX 137 command). The four N–H protons of the macrocyclic complex were located from Δ*F* maps and refined freely subject to an N–H distance constraint of 0.90 Å. Though the N–H proton of the MTBD molecule could be located from a Δ*F* map, it would move into a chemically meaningless position when refined freely, so it was treated as an idealised riding atom with an N–H distance of 0.90 Å.

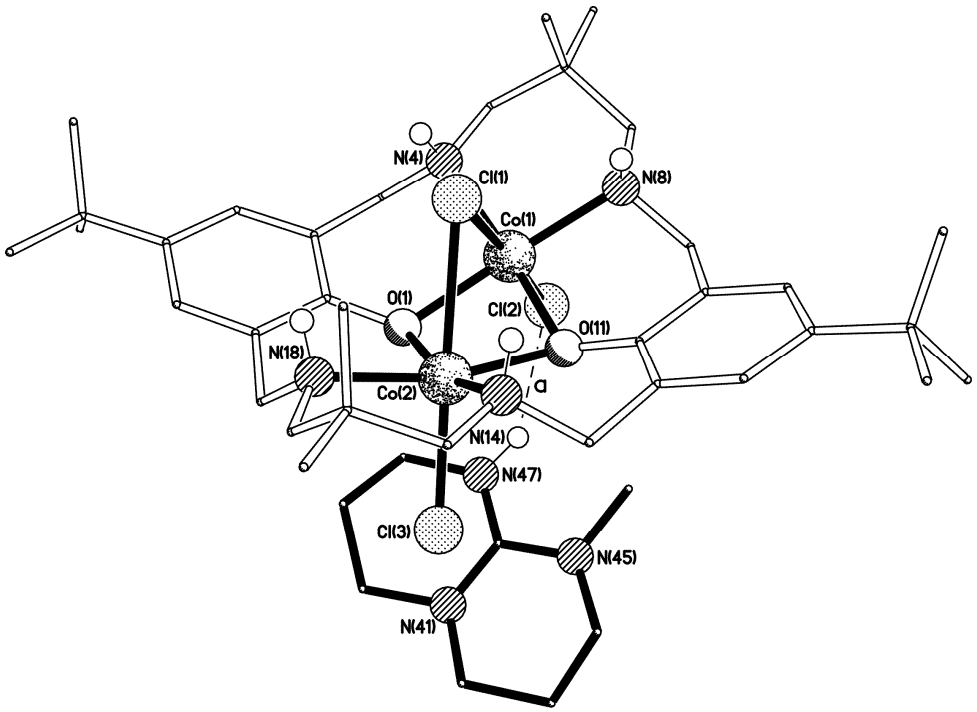

Fig. S11 The molecular structure of **3c**. The N–H···Cl hydrogen bond (**a**) has N···Cl and H···Cl separations of 3.125(3) and 2.33 Å respectively, and an N–H···Cl angle of 148°.

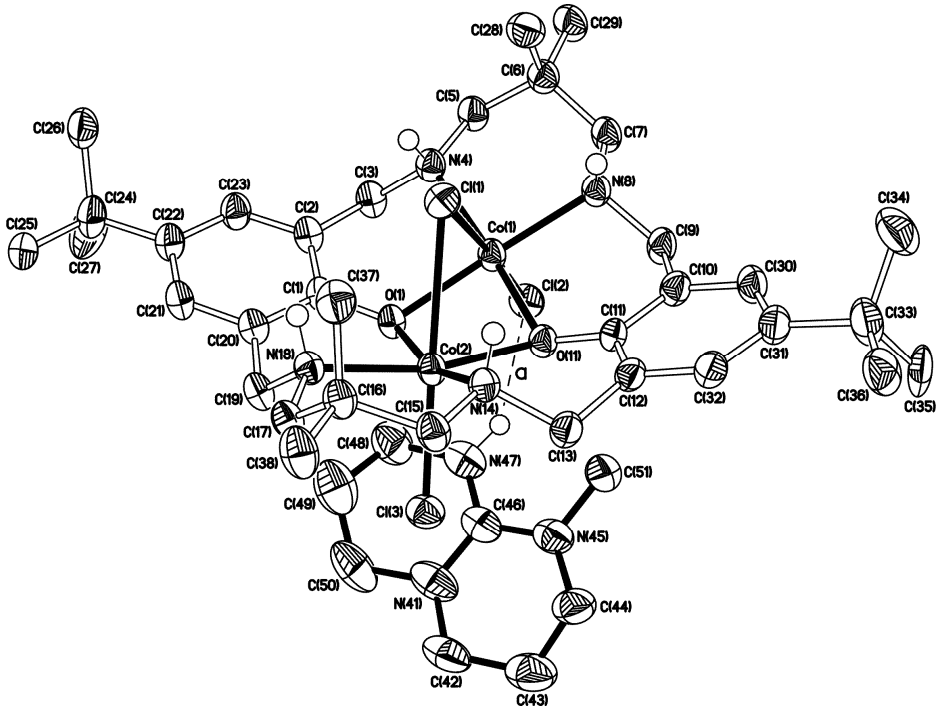

Fig. S12 The molecular structure of **3c** (50% probability ellipsoids). The N–H···Cl hydrogen bond (**a**) has N···Cl and H···Cl separations of 3.125(3) and 2.33 Å respectively, and an N–H···Cl angle of 148°.

Co(1)–Cl(1)	2.6159(7)	Co(1)–Cl(2)	2.4549(7)
Co(1)–O(1)	2.0931(16)	Co(1)–N(4)	2.132(2)
Co(1)–N(8)	2.129(2)	Co(1)–O(11)	2.0985(17)
Co(2)–Cl(1)	2.8077(8)	Co(2)–Cl(3)	2.4095(7)
Co(2)–O(1)	2.0975(17)	Co(2)–O(11)	2.0752(16)
Co(2)–N(14)	2.127(2)	Co(2)–N(18)	2.1349(19)
Co(1)···Co(2)	2.9633(5)		
Cl(1)–Co(1)–Cl(2)	176.91(3)	Cl(1)–Co(1)–O(1)	80.34(5)
Cl(1)–Co(1)–N(4)	88.01(6)	Cl(1)–Co(1)–N(8)	92.78(6)
Cl(1)–Co(1)–O(11)	80.76(5)	Cl(2)–Co(1)–O(1)	97.12(5)
Cl(2)–Co(1)–N(4)	90.33(6)	Cl(2)–Co(1)–N(8)	89.91(6)
Cl(2)–Co(1)–O(11)	100.79(5)	O(1)–Co(1)–N(4)	92.00(7)
O(1)–Co(1)–N(8)	171.23(8)	O(1)–Co(1)–O(11)	83.97(7)
N(4)–Co(1)–N(8)	93.20(8)	N(4)–Co(1)–O(11)	168.55(7)
N(8)–Co(1)–O(11)	89.58(7)	Cl(1)–Co(2)–Cl(3)	178.96(3)
Cl(1)–Co(2)–O(1)	75.76(5)	Cl(1)–Co(2)–O(11)	76.57(5)
Cl(1)–Co(2)–N(14)	87.62(6)	Cl(1)–Co(2)–N(18)	89.85(6)
Cl(3)–Co(2)–O(1)	104.69(5)	Cl(3)–Co(2)–O(11)	102.52(5)
Cl(3)–Co(2)–N(14)	91.89(6)	Cl(3)–Co(2)–N(18)	91.10(6)
O(1)–Co(2)–O(11)	84.43(6)	O(1)–Co(2)–N(14)	163.27(8)
O(1)–Co(2)–N(18)	89.42(7)	O(11)–Co(2)–N(14)	89.94(7)
O(11)–Co(2)–N(18)	166.09(8)	N(14)–Co(2)–N(18)	92.48(8)
Co(1)–Cl(1)–Co(2)	66.126(18)		

Table S6. Selected bond lengths (Å) and angles (°) for **3c**.

The X-ray crystal structure of 4a

Both the C(24) and C(33)-based *t*-butyl groups in the structure of **4a** were found to be disordered. In each case two orientations were identified, of *ca*. 76:24 and 53:47% occupancy respectively. The geometries of all four orientations were optimised, the thermal parameters of adjacent atoms restrained to be similar, and only the non-hydrogen atoms of the major occupancy orientations were refined anisotropically (those of the minor occupancy orientations were refined isotropically). The two included tetrahydrofuran solvent molecules were both found to be disordered. In each case two orientations were identified, of *ca*. 79:21 and 65:35% occupancy for the O(50) and O(60)-based molecules respectively. The geometries of all four orientations were optimised, the thermal parameters of adjacent atoms were restrained to be similar, and only the non-hydrogen atoms of the major occupancy orientations were refined anisotropically (those of the minor occupancy orientations were refined isotropically). The hydrogen atoms of the C(45) methyl group were added in idealised tetrahedral positions and, as they are on an sp^3 centre bonded to an sp^2 centre, the group was allowed to rotate about the C–N bond to find the best fit with the electron density map (the

SHELXL HFIX/AFIX 137 command). Three of the four N–H protons of the macrocyclic complex were located from Δ*F* maps and refined freely subject to an N–H distance constraint of 0.90 Å. The fourth, that bound to N(8), could not be located from a Δ*F* map, and so was placed in an idealised position and then refined freely subject to an N–H distance constraint of 0.90 Å (*i.e.* the same as the others).

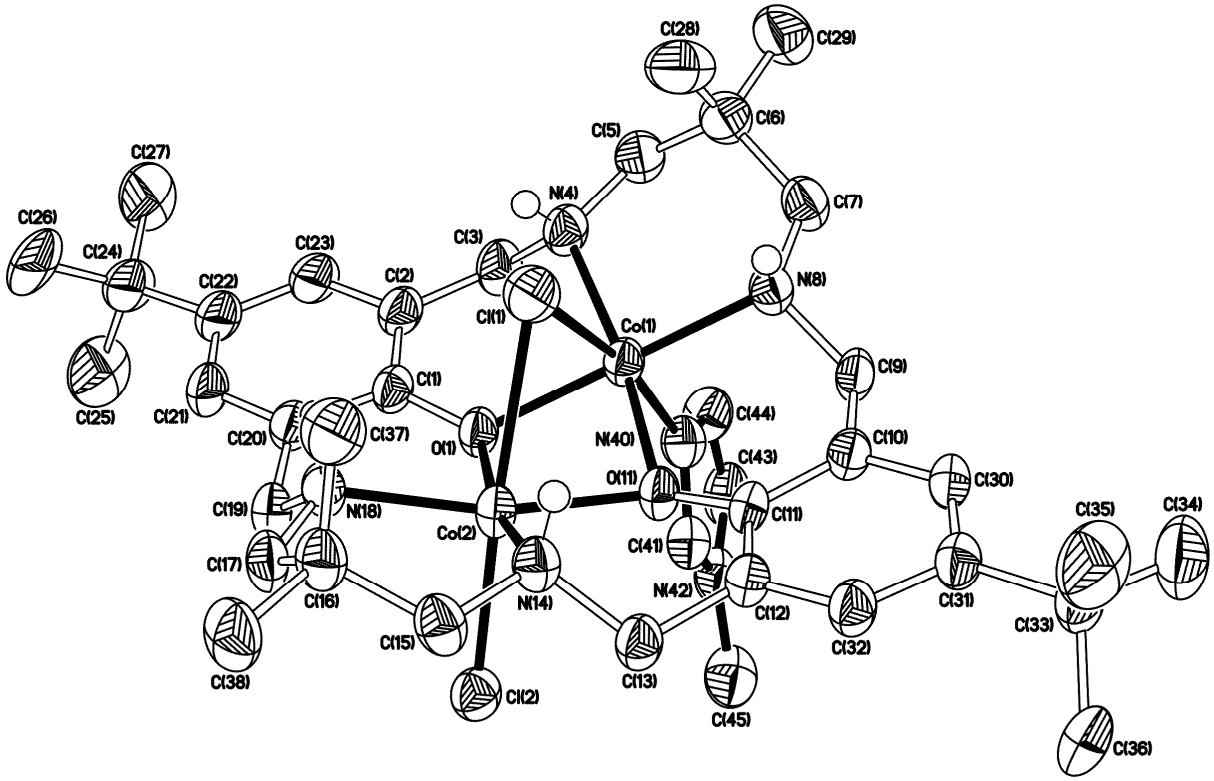

Fig. S13 The molecular structure of **4a** (50% probability ellipsoids).

The X-ray crystal structure of 4b

Both the C(24) and C(33)-based *t*-butyl groups in the structure of **4b** were found to be disordered. In each case two orientations were identified, of *ca*. 72:28 and 86:14% occupancy respectively. The geometries of all four orientations were optimised, the thermal parameters of adjacent atoms restrained to be similar, and only the non-hydrogen atoms of the major occupancy orientations were refined anisotropically (those of the minor occupancy orientations were refined isotropically). The 4.5 dichloromethane solvent molecules per complex were found to be distributed over 6 sites. Three of these are in general positions [those based on C(50), C(55) and C(60)], two are adjacent to C_2 axes [those based on C(65) and C(70)], and one [that based on C(75)] is too close to the C(70)-based molecule to be more than 50% occupancy. The C(50), C(70) and C(75)-based molecules were found to be disordered. Three orientations of *ca.* 64, 27 and 9% occupancy were identified for the C(50)-

based molecule. For the C(70)-based molecule, two orientations of *ca.* 27 and 23% occupancy were identified (two further orientations of the same pair of occupancies are generated by the operation of the C_2 axis). Three orientations of *ca.* 24, 14 and 12% occupancy were identified for the C(75)-based molecule, which can only have a total maximum occupancy of 50% due to its proximity to the site of the C(70)-based molecule. The geometries of all 8 orientations were optimised, the thermal parameters of adjacent atoms restrained to be similar, and only the non-hydrogen atoms of the major occupancy orientations were refined anisotropically (those of the minor occupancy orientations were refined isotropically). The hydrogen atoms of the C(47) and C(48) methyl groups were added in idealised tetrahedral positions and, as they are on sp^3 centres bonded to an sp^2 centre, the groups were allowed to rotate about the respective C–N bonds to find the best fit with the electron density map (the SHELXL HFIX/AFIX 137 command). All four N–H protons were located from ΔF maps and refined freely subject to an N–H distance constraint of 0.90 Å.

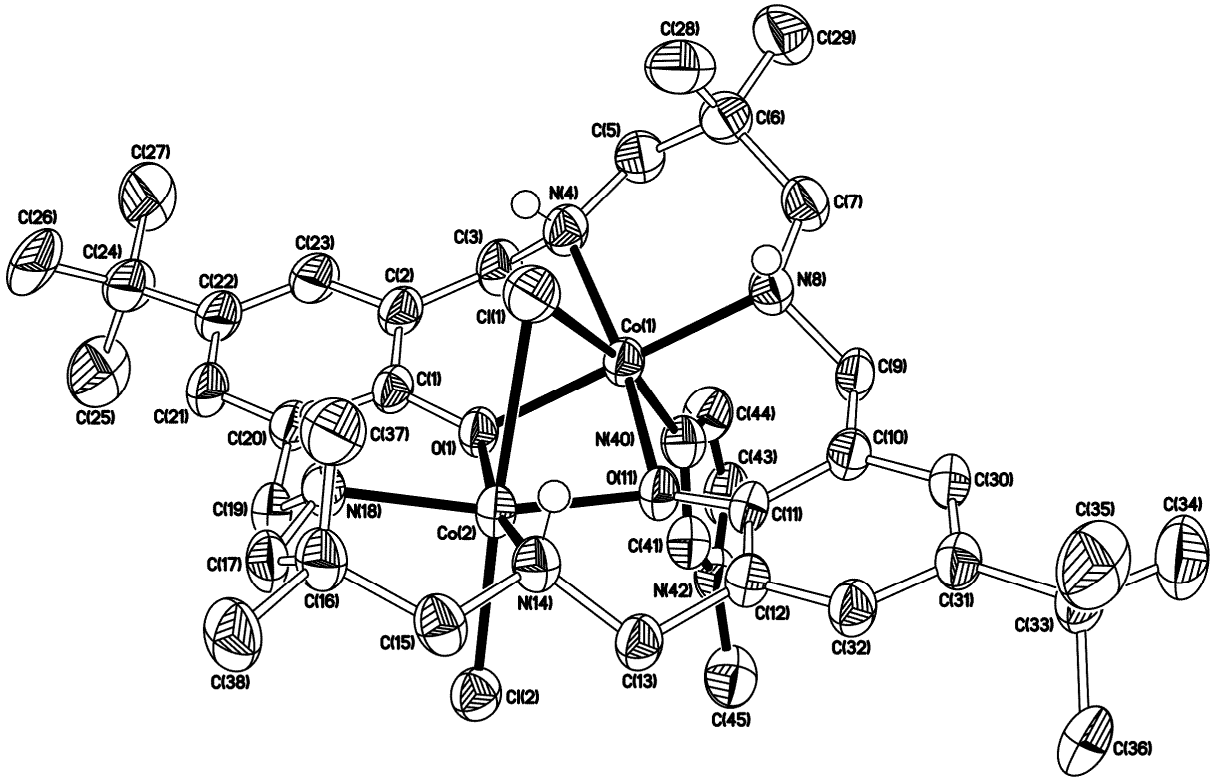

Fig. S14 The molecular structure of **4b** (50% probability ellipsoids).

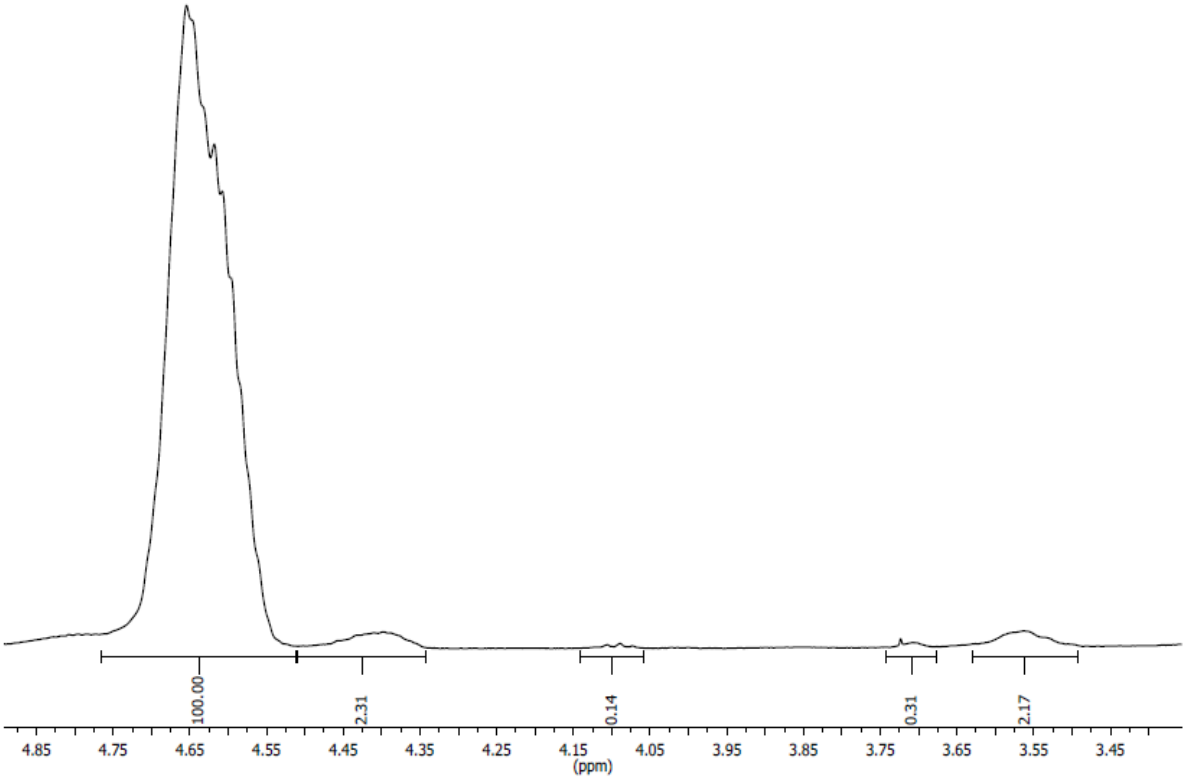

Figure S15: Enhanced ^{1}H NMR spectrum of poly(cyclohexene carbonate) produced by **3c**. Peak at 4.65 ppm corresponds to the methyne protons in carbonate linkages. Peaks at 4.4 and 3.55 ppm correspond to the methyne protons on the end group (OC*H*C_4H_8C*H*OH). Peak at 3.7 ppm is attributed to the methyne proton on the chloride end group.

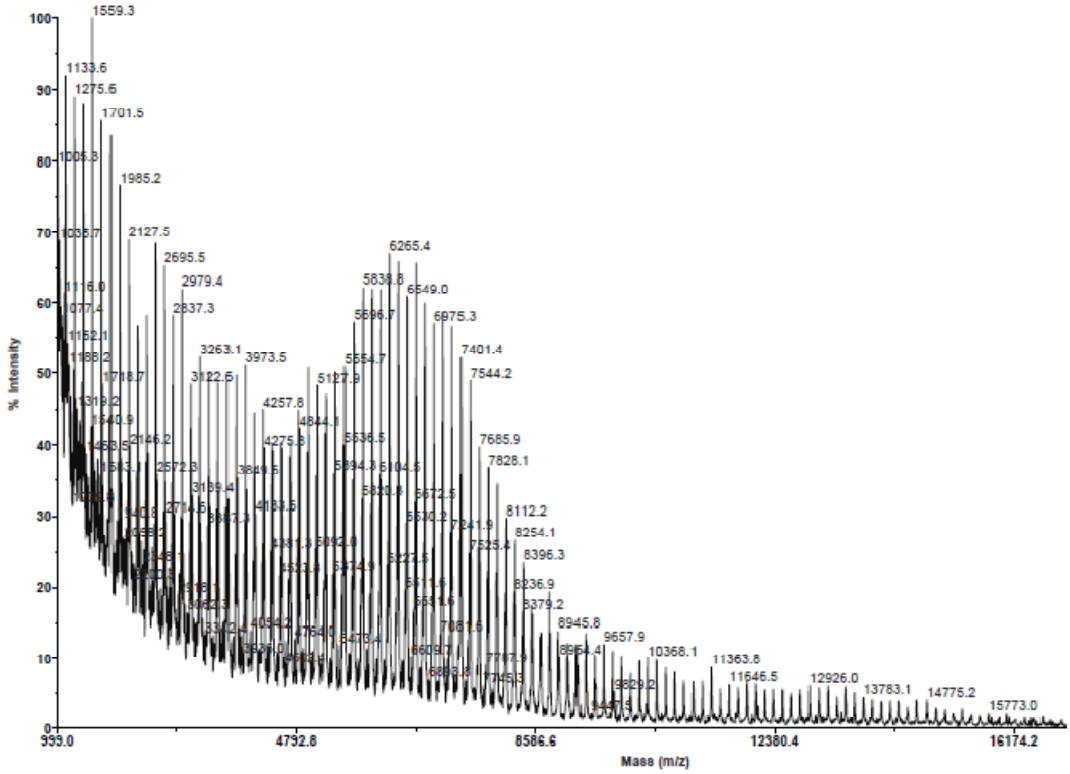

Figure S16: Full MALDI-TOF mass spectrum (top) for PCHC produced by **3a**.

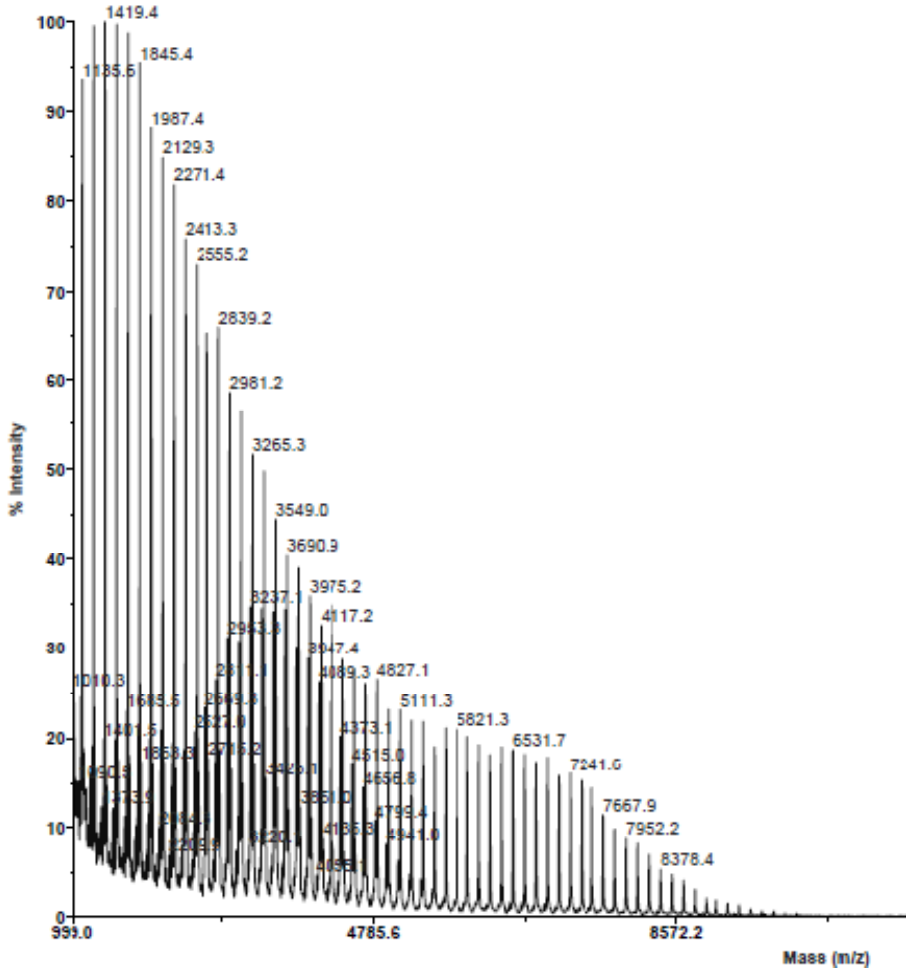

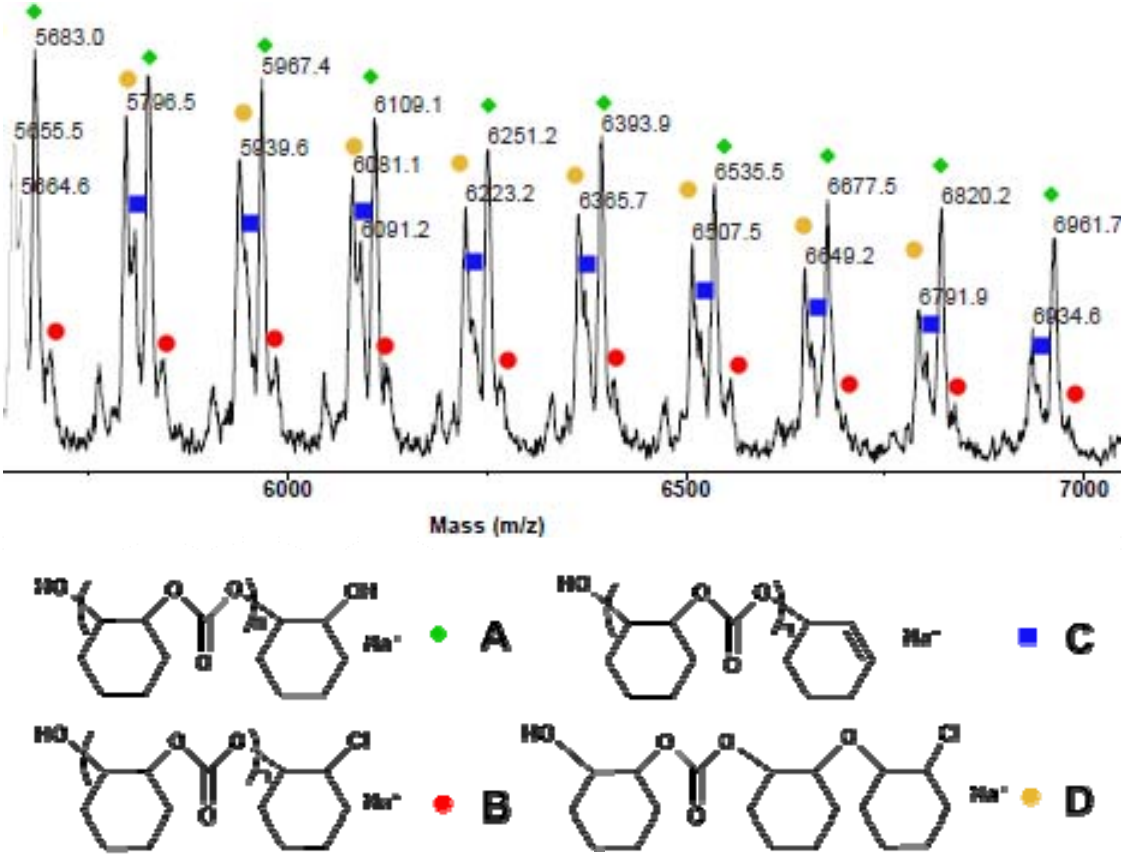

Figure S17: MALDI-TOF mass spectrum and (below) assignment of the end-groups for the PCHC produced by **4c**.

Fig. S18: Additional plots showing the Initial Rate *vs.* $[CHO]_0$ (M), determined by monitoring of ATR-IR absorptions at 1750 (right) and 1285 (left) cm^{-1}.

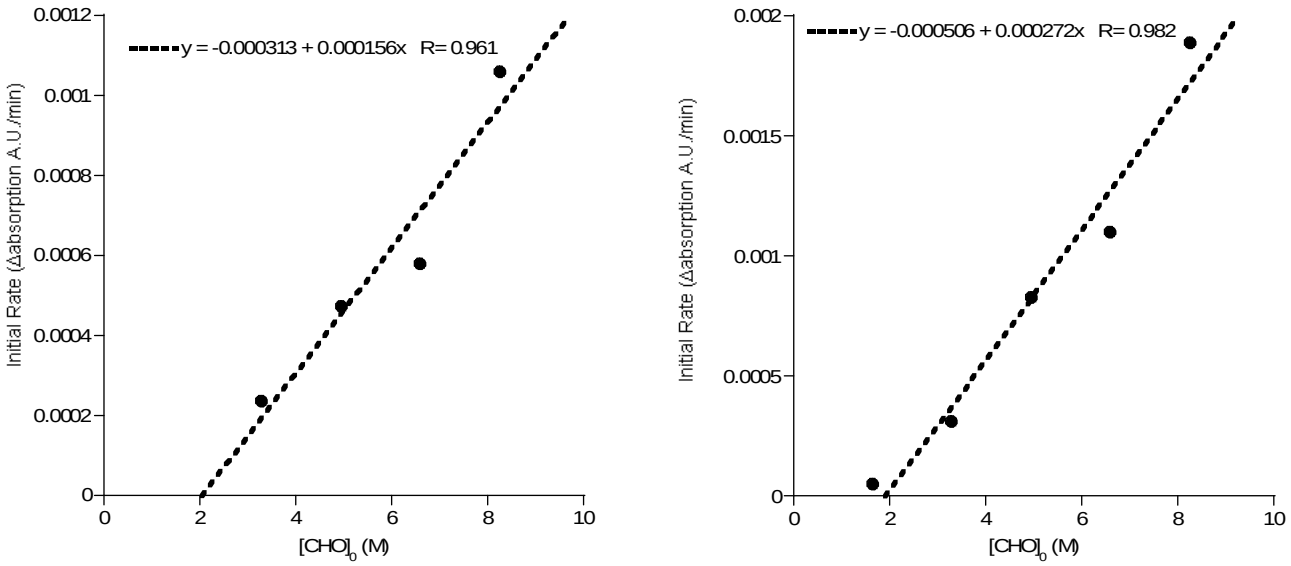

Fig. S19: Additional plots illustrating the Initial Rate *vs.* $[\mathbf{4a}]_0$, determined by monitoring of the ATR-IR absorption at 1285 cm^{-1}.

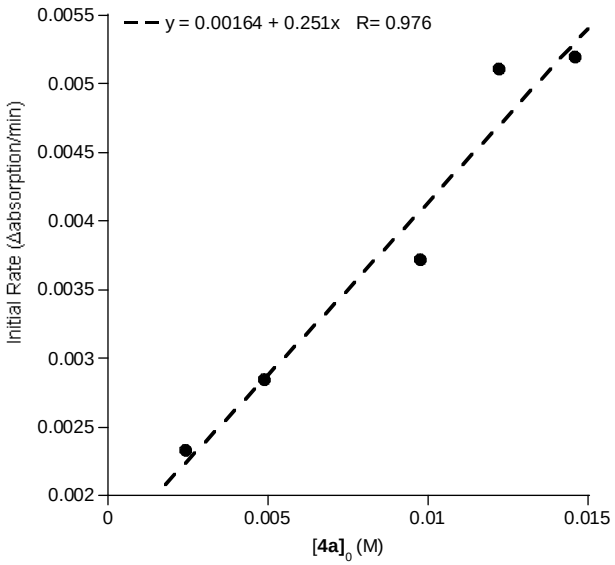

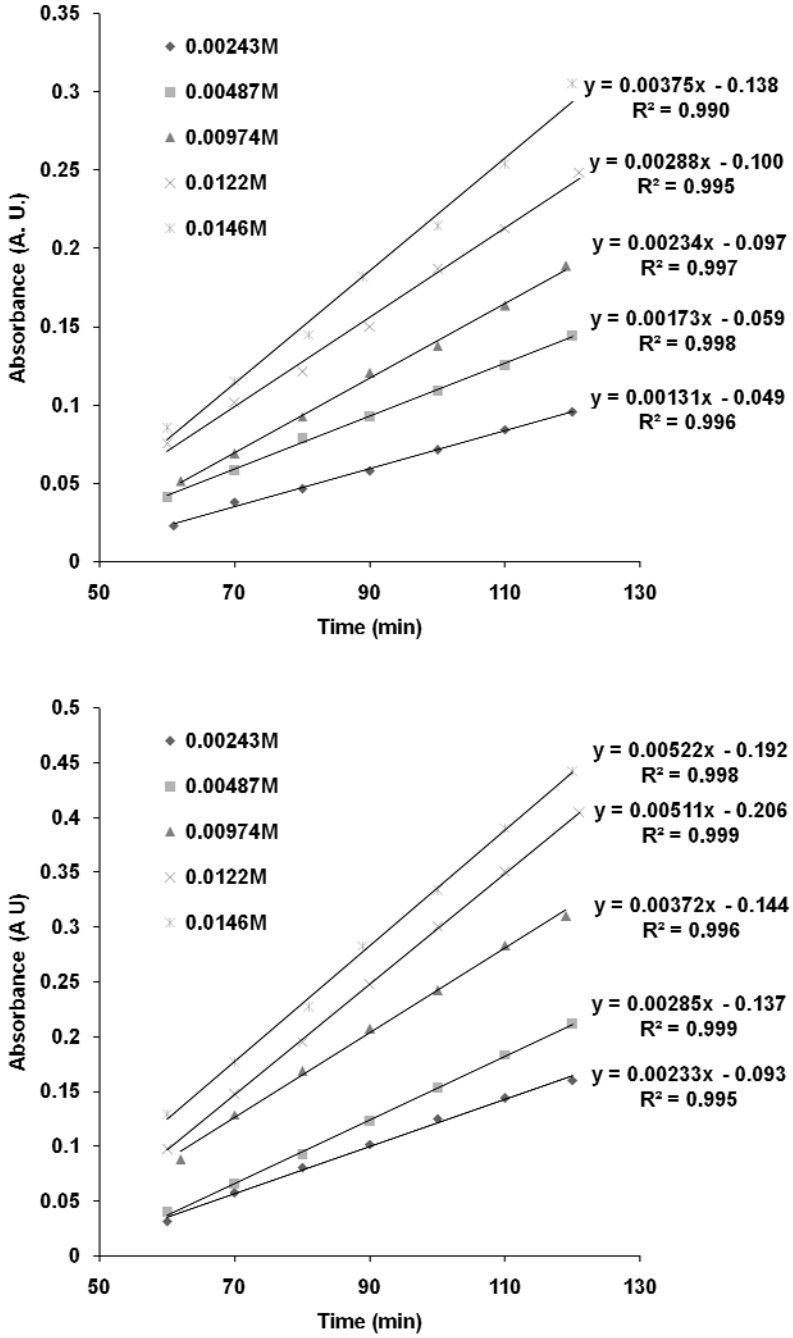

Figure S20: Plots of Absorbance *vs.* Time between 60-120 minutes reaction time with $[\mathbf{4a}]_0$ variation, determined by monitoring of ATR-IR absorptions at 1750 (above) and 1285 (below) cm^{-1}.

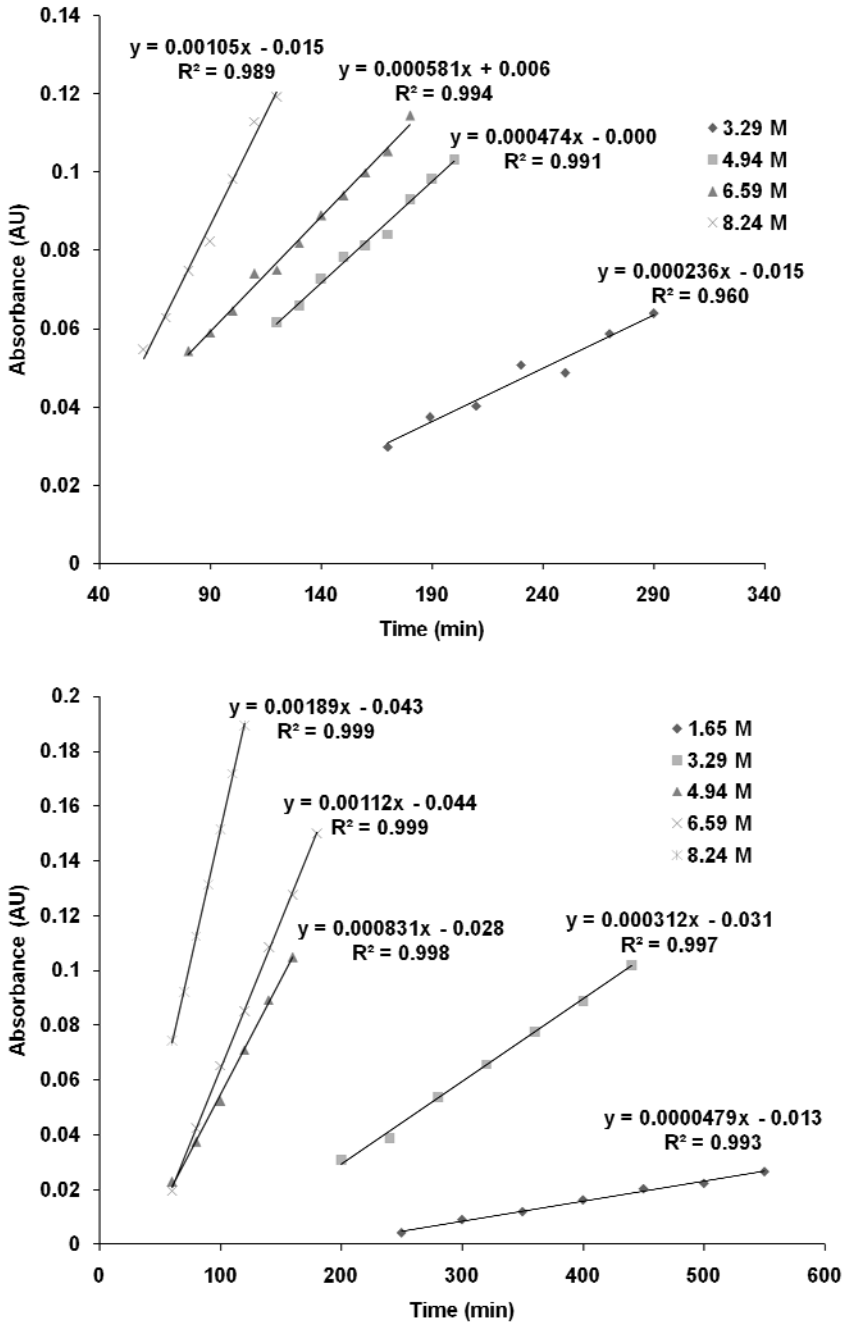

Figure S21: Plots of Absorbance *vs*. Time with [**CHO**]$_0$ variation, determined by monitoring of ATR-IR absorptions at 1750 (above) and 1285 (below) cm^{-1}.

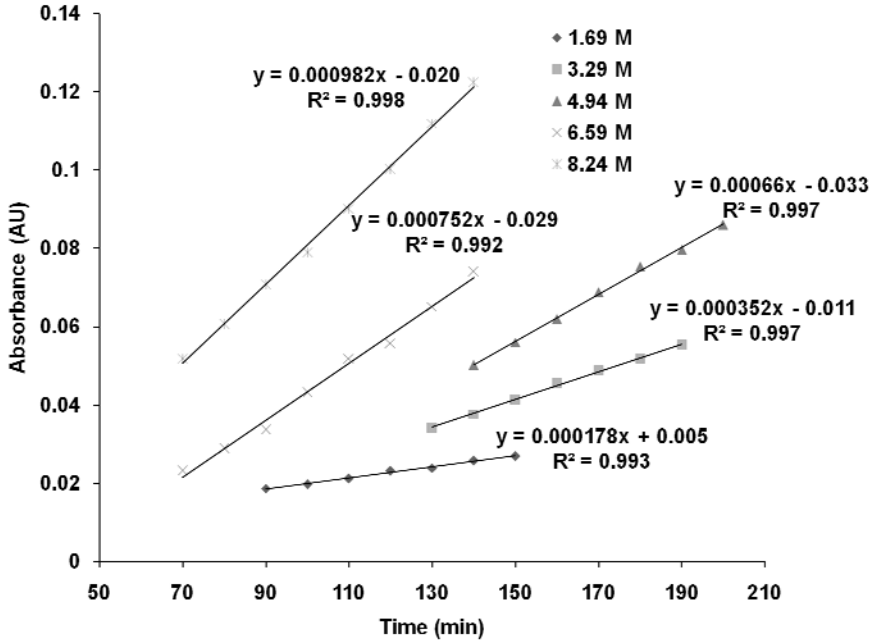

Figure S22: Plot of Absorbance *vs*. Time with [**CHO**]$_0$ variation, determined by monitoring of ATR-IR absorptions at 1050 cm^{-1}.

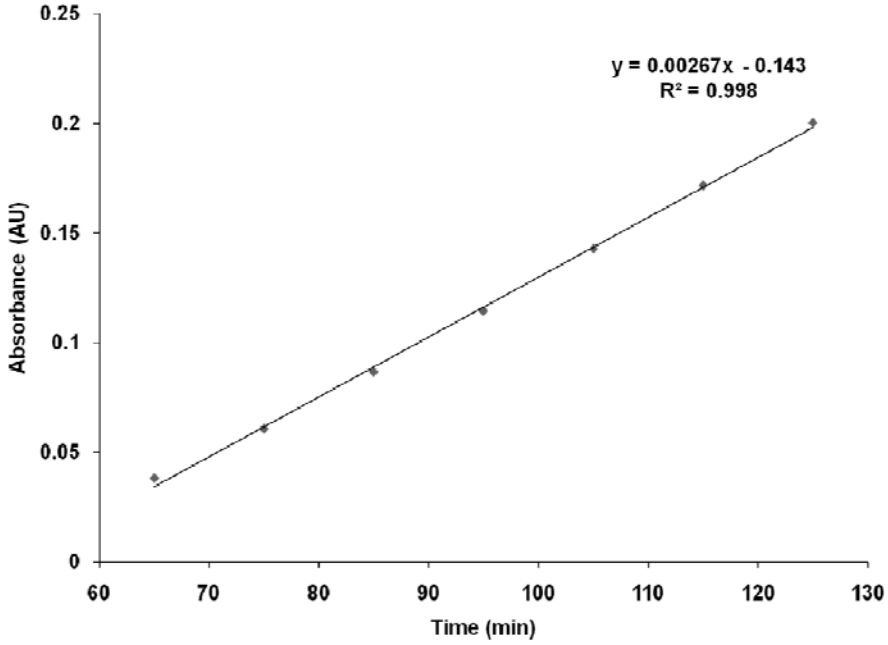

Figure S23: Plot of Absorbance *vs.* Time between 60-130 minutes reaction time with **3a**. Copolymerization conditions: [**3a**]$_0$ = 9.74 mM, in neat CHO, at 80 °C and 1 atm CO_2. Initial rate = 0.00267 AU/min, c.f. 0.00234 AU/min for **4a** under the same reaction conditions.

Complete reference 1a:

Arakawa, H.; Aresta, M.; Armor, J. N.; Barteau, M. A.; Beckman, E. J.; Bell, A. T.; Bercaw, J. E.; Creutz, C.; Dinjus, E.; Dixon, D. A.; Domen, K.; DuBois, D. L.; Eckert, J.; Fujita, E.; Gibson, D. H.; Goddard, W. A.; Goodman, D. W.; Keller, J.; Kubas, G. J.; Kung, H. H.; Lyons, J. E.; Manzer, L. E.; Marks, T. J.; Morokuma, K.; Nicholas, K. M.; Periana, R.; Que, L.; Rostrup-Nielson, J.; Sachtler, W. M. H.; Schmidt, L. D.; Sen, A.; Somorjai, G. A.; Stair, P. C.; Stults, B. R.; Tumas, W., *Chem. Rev.* **2001,** *101*, 953-996.

References

1. Kember, M. R.; Knight, P. D.; Reung, P. T. R.; Williams, C. K., *Angew. Chem., Int. Ed.* **2009,** *48*, 931-933.
2. SHELXTL PC version 5.1, Bruker AXS, Madison, WI, 1997; SHELX-97, G. Sheldrick, Institut Anorg. Chemie, Tammannstr. 4, D37077 Göttingen, Germany, 1998.
3. Kember, M. R.; White, A. J. P.; Williams, C. K., *Macromolecules* **2010,** *43*, 2291-2298.